This is an Accepted Manuscript of a chapter published by Taylor & Francis Group in Hawkins S, Allcock A, Bates A, Firth L, Smith I, Swearer S & Todd P (eds.) *Oceanography and Marine Biology: An Annual Review*. Oceanography and Marine Biology: An Annual Review, 57. Boca Raton, FL, USA: CRC Press, pp. 89-126 on 19 Aug 2019, available online: https://www.crcpress.com/Oceanography-and-Marine-Biology-An-Annual-Review-Volume-57/Hawkins-Allcock-Bates-Firth-Smith-Swearer-Todd/p/book/9780367134150

ESTABLISHED AND EMERGING TECHNIQUES FOR CHARACTERISING THE FORMATION, STRUCTURE AND PERFORMANCE OF CALCIFIED STRUCTURES UNDER OCEAN ACIDIFICATION

SUSAN C. FITZER[1]‡*, VERA BIN SAN CHAN[2, 3, 4]‡, YUAN MENG[4], KENMANI CHANDRA RAJAN[4], SUZUKI MICHIO[5], CHRISTELLE NOT[6], TAKASHI TOYOFUKU[7], LAURA FALKENBERG[8, 9], MARIA BRYNE[10, 11], BEN P. HARVEY[12], PIERRE DE WIT[13], MAGGIE CUSACK[14], K. S. GAO[15], PAUL TAYLOR[16], SAM DUPONT[17], JASON HALL-SPENCER[18], V. THIYAGARAJAN[4]*

[1]*Institute of Aquaculture, Faculty of Natural Sciences, University of Stirling, Pathfoot Building, Stirling, FK9 4LA, UK*

[2]*Department of Biological Sciences, Clemson University, Clemson, SC 29634 USA*

[3] *Ifremer, Physiologie Fonctionnelle des Organismes Marins UMR 6539 LEMAR (CNRS/UBO/IRD/Ifremer) Technopole Iroise - CS 10070 29280 Plouzane, France.*

[4]*The Swire Institute of Marine Sciences and School of Biological Sciences, The University of Hong Kong, Pokfulam, Hong Kong, China.*

[5]*Graduate School of Agricultural and Life Sciences, The University of Tokyo, Tokyo, Japan.*

[6]*Department of Earth Sciences, The University of Hong Kong, Hong Kong, China*

[7]*Japan Agency of Marine Earth Science and Technology JAMSTEC, Department of Marine Biodiversity Research BioDive, Yokosuka, Kanagawa, Japan*

[8]*Norwegian Institute for Water Research NIVA, NIVA Region West, Thormøhlensgate 53 D 5006 Bergen, Norway*

[9]*Simon F.S. Li Marine Science Laboratory, School of Life Sciences, The Chinese University of Hong Kong, Hong Kong*

[10]*School of Medical Sciences, University of Sydney, Sydney, New South Wales, Australia*

[11]*School of Life and Environmental Sciences, University of Sydney, Sydney, New South Wales, Australia*

[12]*Shimoda Marine Research Center, University of Tsukuba, 5-10-1 Shimoda Shizuoka 415-0025, Japan*

[13]*Department of Marine Sciences, University of Gothenburg, 45296 Stromstad, Sweden*

[14]*Division of Biological & Environmental Sciences, Faculty of Natural Sciences, University of Stirling, Cottrell Building, Stirling, FK9 4LA, UK*

[15]*The State Key Laboratory of Marine Environmental Science, Xiamen University, Xiamen, China.*

[16]*Department of Earth Sciences, Natural History Museum, Cromwell Rd, London SW7 5BD, UK.*

[17]*Department of Biological and Environmental Sciences, University of Gothenburg, 45178 Fiskebackskil, Sweden.*

[18]*School of Biological and Marine Sciences, Plymouth University, Plymouth PL4 8AA, Devon, UK*

‡ *shared first-authorship*

**corresponding authors:*

Susan C. Fitzer

e-mail: susan.fitzer@stir.ac.uk

V. Thiyagarajan

e-mail: rajan@hku.hk

Ocean acidification (OA) is the decline in seawater pH and saturation levels of calcium carbonate minerals that has led to concerns for calcifying organisms such as corals, oysters and mussels because of the adverse effects of OA on their biomineralisation, shells and skeletons. A range of cellular biology, geochemistry and materials science approaches have been used to explore biomineralisation. These techniques have revealed that responses to seawater acidification can be highly variable among species, yet the underlying mechanisms remain largely unresolved. To assess the large-scale impacts of global OA, researchers will need to apply a range of tools developed across disciplines, many of which are

emerging and have not yet been used in this context. This review outlines techniques that could be applied to study OA-induced alterations in the mechanisms of biomineralisation and their ultimate effects on shells and skeletons. We illustrate how to characterise, quantify and monitor the process of biomineralisation in the context of global climate change and OA. We highlight the basic principles as well as the advantages and disadvantages of established, emerging, and future techniques for OA researchers. A combination of these techniques will enable a holistic approach and better understanding of the potential impact of OA on biomineralisation and consequences for marine calcifiers and associated ecosystems.

Introduction

The precipitation of minerals such as calcium carbonate ($CaCO_3$) for shells and skeletons using dissolved carbonate and calcium ions is commonly called 'biomineralisation' (Doney et al. 2009). Marine organisms have been producing calcium carbonate biominerals since the Precambrian and the resultant rich fossil record provides insight into the evolution of intricate, orderly and often beautiful structures (Wilkinson 1979). The composition of biominerals varies among taxa and, as the production of shell materials is dependent on the availability of mineral ion resources and on physiological conditions at the site of calcification (Wilbur 1964), mineral composition can reveal how organisms have interacted with environmental conditions over geological time to the present day.

Atmospheric CO_2 levels have increased at a faster rate during the Anthropocene than in any previous time in Earth's history causing a rapid decline in seawater pH and lowering the amount of calcium carbonate minerals (Orr et al. 2005).

Since concerns about OA were first highlighted it has become apparent that CO_2-driven acidification can lead to skeletal abnormalities and slower growth in many marine calcifiers (Hofmann et al. 2008, Vézina and Hoegh-Guldberg 2008, Wittmann and Pörtner 2013). Aragonite, calcite, vaterite (Wehrmeister et al. 2011), and amorphous calcium carbonate which is an important precursor of crystalline carbonate minerals (Addadi et al. 2003), are phases of $CaCO_3$ whose production may be modified by OA. Organisms can be affected by OA as they need to maintain conditions that are

chemically suitable for the process of calcification (supersaturated with calcium [Ca^{2+}] and carbonate [CO_3^{2-}]) or for preventing dissolution (saturation state $\Omega > 1$). Calcite is less susceptible to dissolution at lower pH values than aragonite, unless it contains high levels of magnesium (Ries et al. 2009, Chan et al. 2012). Production of any form of $CaCO_3$ can be energetically expensive (Comeau et al. 2017a) and so the impact of OA on the production and maintenance of $CaCO_3$ structures are modulated by energy acquisition (Melzner et al. 2011) and may be due to by CO_2-driven organism hypercapnia (Byrne et al. 2013).

To capture fully the impact of OA on biomineralisation, several key questions should be addressed. These include questions regarding the direct impact of OA on the process of biomineralisation itself and also about the functional consequences of these changes on shells and skeletons. Resolving these issues requires multidisciplinary research ranging from '–omics' to cell culture, from physiological mechanisms to ecology, and from materials science to crystallography. The complexity of the task is reflected in the plethora of techniques that have been used to investigate biomineralization under OA conditions, including buoyant weight, total alkalinity anomality, total calcium content, annual estension, calcein labelling and the use of radio isotopes (Table 1). This diversity of approaches allows investigators to tackle different questions related to the impact of OA on the process of biomineralisation, although there is a need to understand how different techniques compare when measuring similar processes (Schoepf et al. 2017). The selection and refinement of a technique is dependent upon scientific question and practical aspects related to the study question, experimental design and biological models (Figure 1).

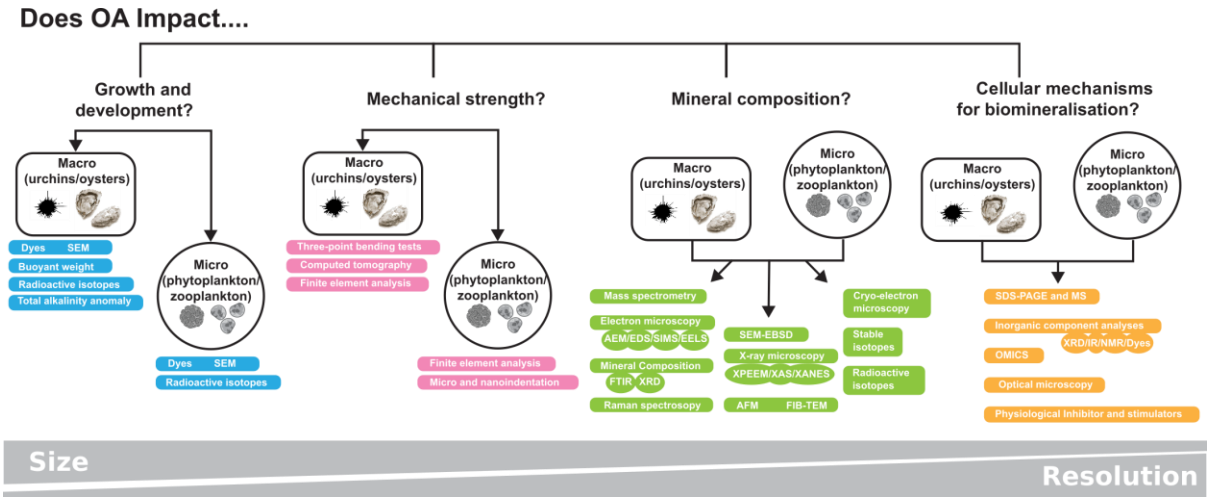

Figure 1. A schematic representation of analytical methods studying whole animal growth and development (in blue), mechanical strength (in pink), mineral composition (in green), and cellular mechanisms of biomineralisation (in orange) that enables the answering of various level of questions. These techniques can be strategically applied to macrobiota (e.g. urchin or oysters) or microbiota (e.g. phytoplankton or zooplankton). From left to right, the figure shows the techniques applicable to smaller scale samples with increasing resolution. At a lower resolution, macrobiota can be measured in terms of various shell growth and development parameters (in blue) and mechanical properties, while some approach has more limitations with microbiota. At a high resolution, microbiota and macrobiota can be studied for their shell structure (in green) and cellular mechanisms for biomineralisation (in orange).

Here we review an array of techniques used to explore the consequences of rising global CO_2 levels on biomineralisation in marine organisms. We organize the techniques by categorizing the biological or mineralogical parameters of interest. We evaluate their advantages and disadvantages so that future work can more effectively measure the effects of OA on biomineralisation . We also highlight recent advances in the study of the effects of ocean acidification on biomineralisation and how interdisciplinary collaboration can advance the field.

Growth and development

When evaluating the impact of OA on biomineralisation, it is important to discriminate between methods measuring gross and net calcareous shell growth as the product of biomineralisation (Figure 2). The term ‘gross calcification’ refers to the biologically controlled process of $CaCO_3$ production through the formation of $CaCO_3$ minerals from a super saturated solution ($CaCO_3$ precipitation). In contrast, the term ‘net calcification’ is the net effect of gross calcification and dissolution (Cyronak et al. 2016). $CaCO_3$ dissolution or decalcification is the dissolution of $CaCO_3$ minerals in an under saturated solution. These processes combine to influence net calcification; for example, the upregulation in gross calcification rates of the limpet *Patella caerulea* helps to counteract higher shell dissolution rates (Rodolfo-Metalpa et al. 2011).

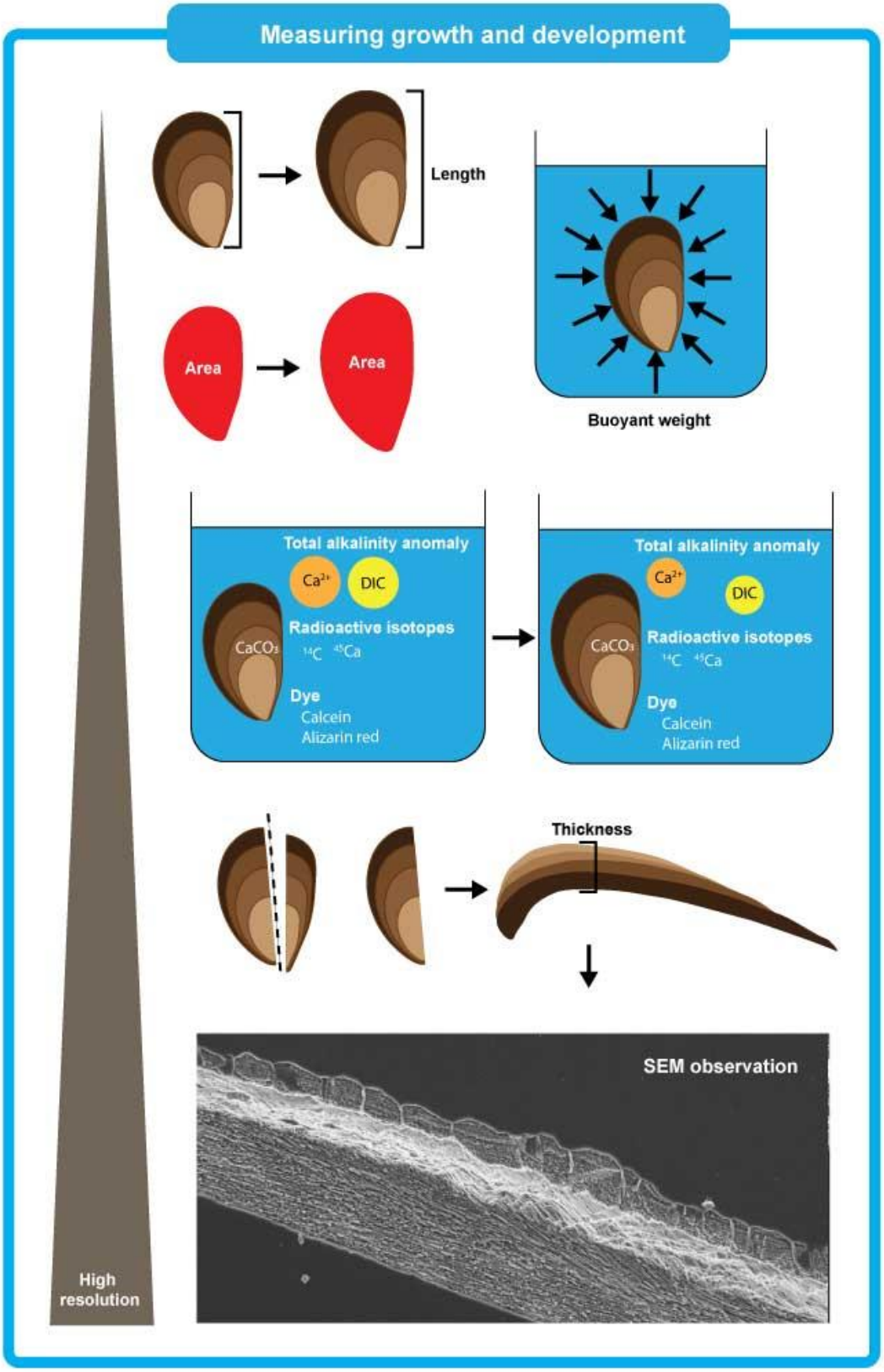
Measuring growth and development
Length
Area
Area
Buoyant weight
Total alkalinity anomaly
Ca2+
DIC
CaCO3
Radioactive isotopes
14C 45Ca
Dye
Calcein
Alizarin red
Total alkalinity anomaly
Ca2+
DIC
CaCO3
Radioactive isotopes
14C 45Ca
Dye
Calcein
Alizarin red
Thickness
SEM observation
High resolution

122

Figure 2. Schematic representation of techniques for measuring growth and development in biomineralising organisms. The tapering bar on the left indicates the changing level of resolution for each technique. From top to bottom, growth and development can be measured on whole shells and skeletons using techniques such as length and buoyant weight measurements. More sensitive techniques are represented in the middle for the use of dyes, radioactive isotopes and total alkalinity anomaly technique. At the bottom of the figure, sectional surface of a shell at higher resolution can be visualized and thickness can be measured using techniques such as SEM microscopy.

Dyes

A range of chemical dyes (e.g. alizarin red, calcein) are used to mark shells or exoskeletons to assess growth over time and have been used in OA studies to determine the impact on calcification in corals, coralline algae and bivalves (Rodolfo-Metalpa et al. 2011, Dickinson et al. 2012a, Tambutté et al. 2012, Bradassi et al. 2013, Venn et al. 2013, Fitzer et al. 2014b, Fitzer et al. 2015b). Calcein labelling is often preferable because calcein was found better incorporated into foraminiferan calcite and emitted fluorescence more strongly than the other markers such as Alizarin complexone, oxytetracycline, and xylenol orange (Bernhard et al. 2004). Calcein has been applied in OA research to assess coralline algal, coral and mollusc growth during experiments (Dickinson et al. 2012b, Bradassi et al. 2013, Venn et al. 2013, Fitzer et al. 2014b, Fitzer et al. 2015b). The techniques are low cost, less invasive as compared to sacrificial shell sampling and the results are readily comparable.

SEM

Abnormalities and morphology can be assessed by optical microscopy. However, scanning electron microscopy (SEM) is required for high resolution characterisation of biomaterial microstructures and has been used to show modified skeletal phenotypes in a range of species grown under OA conditions (Riebesell et al. 2000, Orr et al. 2005, Iglesias-Rodriguez et al. 2008, Lombardi et al. 2015). The

advantage of this approach include the ability to assess shape and malformation in net growth, while the disadvantages include higher costs and an extended preparation time.

When evaluating net shell growth as the overall product of biomineralisation, one of the simplest and most widely used methods to approximate net calcification is shell and exoskeleton length, as it is both non-invasive low-cost. However, this approach can fail to reveal impacts on gross and net calcification not expressed in the overall structure of the skeleton. For example, OA can cause skeletal malformations which can only be identified by microscopy (Langdon et al. 2000, Reynaud et al. 2003, Langdon and Atkinson 2005, Gazeau et al. 2007, Cooper et al. 2008, Jokiel et al. 2008, Ries et al. 2009). This can be partly addressed by including morphometric parameters to resolve shapes, and thickness, for example using 3-dimensional measurements generated from computed tomography (Rühl et al. 2017). It is therefore important to consider the net growth of the whole shell or skeleton.

Skeletal growth assessed as annual extension rate (cm^2 yr^{-1}) is commonly used to determine growth rates of calcareous red algae and corals (Marsh 1970), with recent research applying photogrammetric methods based on digital photography and advanced image processing techniques for non-destructive measurements of area and volume (Mackenzie et al. 2014, Norzagaray-López et al. 2017). Densitometry using X-rays (Table 2) assesses the density of calcified structures (Carricart-Ganivet and Barnes 2007) and has been used to identify growth bands and to calculate growth rates of individuals or colonies (Cooper et al. 2008).

Buoyant weight

To monitor changes in mineral content, buoyant weight determined by immersion is frequently used (Davies 1989, Herler and Dirnwöber 2011). Correction for seawater salinity and temperature variation between measurements is necessary (Fang et al. 2013). The buoyant weight technique is non-invasive (Molina et al. 2005) and remains one of the most common techniques to determine net calcification rate in OA studies, especially in corals (Herler and Dirnwöber 2011). Such an approach has shown that an array of temperate corals *Oculina arbuscula*, pencil urchins *Eucidaris tribuloides*, hard clams *Mercenaria mercenaria*, conchs *Strombus alatus*, serpulid worms *Hydroides crucigera*, periwinkles

174 *Littorina littorea*, bay scallops *Argopecten irradians*, oysters *Crassostrea virginica*, whelks *Urosalpinx*
175 *cinerea*, and soft clams *Mya arenaria* show mixed responses to CO_2-induced acidification, thereby
176 highlighting the complexity of biomineralisation responses (Ries et al. 2009).

177 *Radioactive isotopes*

178 Naturally occurring radioactive isotopes can be used to measure growth by spiking organisms with a
179 radiotracer (Sabatier et al. 2012). Liquid scintillation counting is used to amplify the signal and
180 quantify the amount or rate of ^{45}Ca being incorporated into the biomineral structure (Rodolfo-Metalpa
181 et al. 2011, Rodolfo-Metalpa et al. 2015). ^{45}C is a non-natural radioactive isotope, therefore any changes
182 in ^{45}Ca quantity represents shell material accretion or loss by the calcification process that occurs during
183 the experiment and prior calcification is not taken in account (Furla et al. 2000). Similarly, synthetic
184 radioactive ^{14}C isotopes enable the measurement of carbon flux related to photosynthesis and
185 calcification (Guo et al. 2009, Li et al. 2015). The ^{45}Ca technique has been used in OA research to
186 determine the impact of increasing pCO_2 levels on cold-water corals, suggesting that calcification is not
187 disrupted under OA (Rodolfo-Metalpa et al. 2015). Gross calcification rates have been quantified using
188 ^{45}Ca in corals, limpets, mussels, foraminifera, coccolithophores and oyster larvae (McEnery and Lee
189 1970, Erez 1978, Satoh et al. 2009, Rodolfo-Metalpa et al. 2011, Rodolfo-Metalpa et al. 2015, Frieder
190 et al. 2016). In contrast, ^{14}C has mainly been applied in unicellular organisms such as coccolithophores
191 (Paasche 1963, Nimer and Merrett 1993, Gao et al. 2009), foraminifera (ter Kuile et al. 1989), and
192 diatoms (Li et al. 2015). Advantages include the improved spatial resolution, taking into account
193 material accretion during the incubation period. However, a major disadvantage of this technique is the
194 destructive nature of sampling unlike other techniques such as buoyant weight to determine calcification
195 rates.

196 *Total alkalinity anomaly technique*

197 Net calcification rate can be measured by determining the amount of $CaCO_3$ taken up by an organism
198 (Gazeau et al. 2007). When an organism precipitates a mole of $CaCO_3$ it takes up two moles of HCO_3^-,
199 thereby reducing the alkalinity of the surrounding seawater over the incubation period (Langdon et al.

2000, Langdon and Atkinson 2005, Gazeau et al. 2007). The total alkalinity anomaly technique has been used as an alternative to the buoyant weight method to determine net calcification rates in a range of calcifying organisms including corals, mussels and oysters (Langdon et al. 2000, Langdon and Atkinson 2005, Gazeau et al. 2007). A recent study recommends that the technique is more suitable for shorter term (e.g. day/night) incubations whereas the buoyant weight method is suitable for longer term studies when resources are limited (Schoepf et al. 2017). Less frequently, calcium content has been determined directly using mass spectrometry as a proxy for calcification (Wood et al. 2008). Both the total alkalinity anomaly and the buoyant weight techniques are low cost and take into account skeleton malformations, however there is variability between incubation methods. Promisingly, there is agreement in the results obtained from the different methods, with the major trend of a reduction in net biomineralisation under OA shown by both techniques (Langdon et al. 2000, Langdon and Atkinson 2005, Gazeau et al. 2007).

Mechanical tests - Protective function or ability to survive

OA impacts the gross and net calcification in many marine calcifiers, and therefore it would be expected that OA would similarly impact the function of the shell or skeleton. Mechanical properties of shells/skeletons can be quantified by two parameters: a) hardness (resistance to irreversible deformation) and b) compressive strength (force needed to induce cracking). These parameters can be used to evaluate the functional impacts of changes in biomineralisation under OA. For example, changes in these parameters have implications on the vulnerability of reef-forming species and associated ecosystems, as well as consequences for predator-prey interactions (Fu et al. 2016).

Three-point bending tests

As a classical, simplistic and low cost approach to examine mechanical features of brittle biomineral structures, three-point bending tests measure the flexural strength and modulus and commonly used to define material properties in its ability to resist bending. Three-point bending tests have been applied to measure the stiffness of the ambital plates in sea urchins grown in OA and found that there can be no significant impact on the protective function of the exoskeleton (Collard et al. 2016). Purpose-made

devices consisting of two supportive beams with appropriate span length and a loading beam can be built according to the specific morphology of the biomineral sample (Guidetti and Mori 2005, Asnaghi et al. 2013). These tests provide relevant information to the protective function of the shell or exoskeleton. The flexural response to a three-point bending test device mimics the deformation response to predatory attack by fish (Guidetti and Mori 2005). This exoskeleton robustness test was applied in the OA study of a sea urchin, and revealed increased pCO_2 reduced the defense of a sea urchin to the predator (Asnaghi et al. 2013). If samples are to be directly compared, it is essential to first standardize the thickness and sectional area of the test material, which requires additional preparation time to ensure the biomineral samples are cut into a standard size. The three-point bending tests have the advantage of being able to measure the whole structure mechanical response; disadvantages are that it can be time consuming as purpose-made devices may be required for unusually shaped shell structures.

Computed tomography

Computed tomography (CT) and micro-computed tomography (Micro-CT) are powerful, non-destructive techniques to evaluate biomineralised structures. Micro-CT allows 3D visualisation of X-ray image series generated by scanning with axial rotation in small steps. This method enables examination of internal structural features at fine spatial resolution (Li et al. 2016). A micro-CT dataset allows a variety of quantifiable measurements, including thickness in terms of pixel distance, volume in terms of voxel counts and density in terms of brightness of each pixel at higher resolution compared to CT (Fantazzini et al. 2015, Tambutté et al. 2015, Chatzinikolaou et al. 2017).

With these 3D geometric morphometrics and measurements, the growth rate, density and morphological changes due to OA can be investigated. Micro-CT has been applied in OA studies on gastropods (Chatzinikolaou et al. 2017), tubeworms (Li et al. 2014, Li et al. 2016), and shrimp (deVries et al. 2016) to infer changes in the protective function of the exoskeletons. 3D model visualisation also enables the analysis of density distribution to understand the engineering of calcareous structures. Consequently, the presence of structurally vulnerable regions can be identified. Micro-CT analysis has been used in OA to determine the survival of coral through protective exoskeleton function (Tambutté et al. 2015).

253 Exoskeleton porosity often represents shell protective function. In particular, intertidal gastropods
254 *Nassarius nitidus* and *Columbella rustica* exhibited density reduction in acidified conditions
255 (Chatzinikolaou et al. 2017) while coral skeletons also showed an increased porosity at lower pH
256 through micro-CT (Fantazzini et al. 2015, Tambutté et al. 2015).

257 The spatial resolution of most medical micro-CT is sufficient to provide a good measurement for large
258 calcifiers, and typically have a resolution of 15 - 1000 μm per pixel. As a consequence, however,
259 observation of marine plankton and larvae remains as a challenge. Another limitation of micro-CT is
260 the detection sensitivity which can generate false negatives through thin minerals where regions may
261 appear as empty space in the 3D reconstruction. Therefore, it is important to verify the representative
262 morphology by combining micro-CT with an SEM approach. All density measurements should be
263 calibrated with a standard material which has a known bone mineral density (BMD, $g.cm^{-3}$) in terms of
264 calcium hydroxyapatite and its corresponding pixel intensity for each scan (Li et al. 2014). Since there
265 are no commercially available standards for calcium carbonate calibration, density measurements are
266 relative and has limited comparability with other studies.

267 *Finite element analysis*

268 The field of engineering and computational simulation can be applied creatively to understand structural
269 impacts to biominerals caused by OA. In a simulation, any weakness in the architecture is highlighted
270 and the loading capacity can be calculated from the shape and empirical data (Li et al. 2016). Therefore,
271 the application of structural analysis can be performed when shapes and mechanical properties of the
272 biological mineral are both known, providing a holistic picture of how well each calcified material
273 functions as the protective or supportive structure.

274 The most widely applied numerical tool for computational simulation is finite element analysis (FEA)
275 (Li et al. 2014; Li et al. 2016). To solve a problem using FEA, the problem is divided into smaller and
276 simpler parts which are called finite elements. By assembling the solution of all finite elements
277 mathematically, a total approximate solution of the large problem can be obtained. FEA enables the
278 mechanical behaviours of complex biomineralised structures to be investigated accurately. The FEA

279 can include the different experimental mechanical properties, such as elasticities of different
280 components of the shell structure, as well as simulate the effects of loading, for example the crushing
281 forces associated with a predator attack.

282 With the diverse calcareous structures being produced by marine organisms, FEA can be applied to
283 assess changes in mechanical performances due to morphological changes. For example, FEA has been
284 applied to understand the mechanical response of a tubeworm under OA combined with low salinity
285 and warming treatments. This enabled the identification of the most vulnerable region of the tube and
286 the highest risk of fracture failure under predatory attack (Li et al. 2014, Li et al. 2016). This
287 demonstrates that FEA can be developed as biologically accurate model to determine the impact of OA
288 on the protective function of calcareous shells and exoskeletons. Beside its advantage, FE models
289 especially when it is 2-D simplified (Ragazzola et al. 2012), often fail to account for heterogeneity,
290 malformation and shape changes. In addition, 3-D models are complex and requires advanced
291 computational efforts (Melbourne et al. 2015).

292 *Micro- and nanoindentation*

293 Biominerals are composed of mineral crystals and an organic matrix framework. As a result, biogenic
294 calcite has been reported to be 50-70% harder than geological calcite (Kunitake et al. 2012, Kunitake
295 et al. 2013). Due to the high heterogeneity in morphology, structure and composition of mineralized
296 shells and exoskeletons, hardness has been widely used as a comparable evaluation of mechanical
297 properties (Beniash et al. 2010, Dickinson et al. 2012a, Fitzer et al. 2015b).

298 The strength of biomineralised structures can be characterised by a crushing or compressive test where
299 machine applies and reads compressive force- versus displacement. The entire structure of specimens
300 can be used to mimic a predatory attack (Byrne et al. 2014). However, biomineralised structures are
301 typically not homogenous and using a single point allows a better mechanical understanding of the shell
302 property.

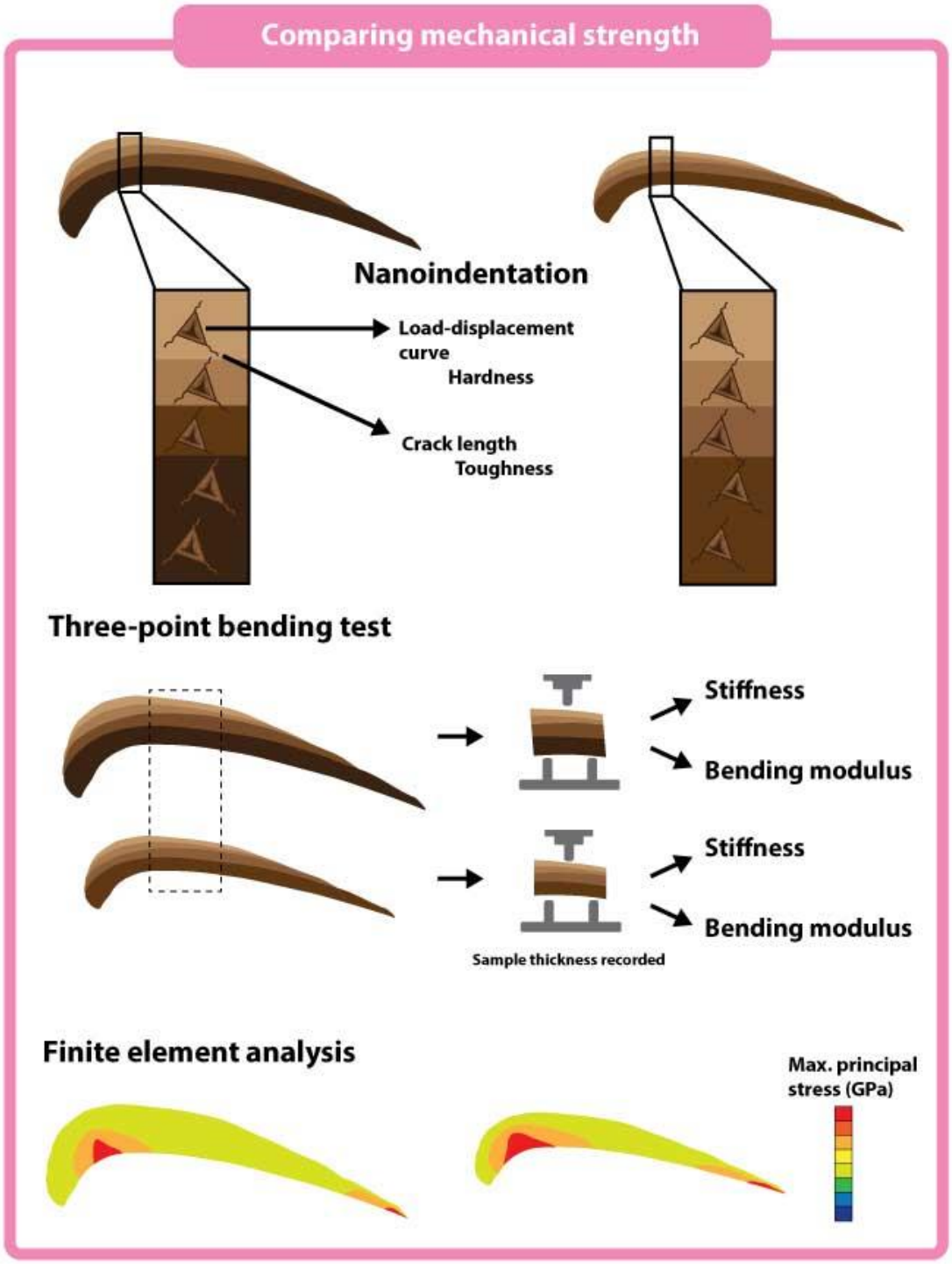

303

304 **Figure 3. Schematic representation of techniques to compare mechanical properties in**
305 **biomineralizing organisms. Nanoindentation and 3-point bending are two highlighted techniques**
306 **for assessing mechanical properties including hardness, elasticity, fracture toughness and stiffness**

of biominerals. Micro and nanoindentation in combination of computed tomography and finite element analysis project the impact of OA on mechanical properties of shells and skeletons during predatory attacks.

Two main methods can be used to understand the impact of OA on shell mechanical properties (Figure 3): 1) microhardness tests can measure Vickers hardness numbers (HV) determined by the ratio of the force applied by the indenter and the surface area of the final indent (Beniash et al. 2010, Dickinson et al. 2012a); and 2) nanoindentation which can measure the hardness and elasticity in a single indent. With the development of a depth-sensing indenter, the hardness and elastic modulus (a measure of stiffness) in units of pascals (Pa) from each indentation can be obtained from the loading-unloading curve by using the Oliver-Pharr model (Oliver and Pharr 1992). This method enables the measurement of shell hardness and has been used to address how the protective function of several mollusc species grown under experimental OA might be affected (Beniash et al. 2010, Dickinson et al. 2012a, Fitzer et al. 2015b). The results indicate no significant impact on microhardness in clams (Beniash et al. 2010) and oysters (Dickinson et al. 2012a) but an increase in microhardness in mussels (Fitzer et al. 2015c).

The advantage of nanoindentation is its precision at the nanometre scale. Nanoindentation enables spatial refinement where the mechanical properties profile can be examined (Li et al. 2014). At finer spatial resolution, mechanical features can be associated with the different textures of the mineral (Goffredo et al. 2014). The influence of OA can be reflected in different mineralised layers or structures of the marine invertebrate shell. Nanoindentation enables substantial refinement, for example, the hardness and modulus of the tubeworm from the exterior to the interior were mapped by nanoindentation in order to address questions about the protective function of the structure (Li et al. 2014, Fitzer et al. 2015b). The mechanical properties of the exterior to the interior portion of the tube were shown to decrease under OA compared to the middle portion of a tubeworm (Li et al. 2014). Researchers can analyse the same polished sample using SEM, allowing correlation between structural alteration and mechanical performance. This has been done for mussels (Fitzer et al. 2015b) and

tubeworms (Chan et al. 2012, Li et al. 2014) grown in OA for extended periods of time showing that OA-induced structural alteration may lead to deteriorations in mechanical performance. Both hardness tests have the disadvantage of requiring a highly polished sample surface (Perez-Huerta and Cusack 2009) and sample preparation can be both time-consuming and challenging (Milano et al. 2016).

In addition to hardness, the dimensions of the cracks generated around the indent can be used to determine the fracture toughness combined with the elasticity of the material as shown for bivalves grown under OA conditions (Beniash et al. 2010, Dickinson et al. 2012a, Fitzer et al. 2015b). By measuring the lengths of cracks, the plane-strain fracture toughness (KIC) can be calculated (Lawn et al. 1980, Anstis et al. 1981). However, it is difficult to define the local and bulk fracture behaviours by this technique, which makes it problematical to determine the accuracy of the fracture toughness values given by indentation (Kruzic et al. 2009). This technique has enabled the determination of the impact of OA on shell protective function: the fracture toughness of oyster shells and mussel shells was reduced (as measured by microhardness tests), which confirmed that the calcite shell became more brittle in OA conditions (Beniash et al. 2010, Dickinson et al. 2012a, Fitzer et al. 2015b).

Mineral composition - Biomineralisation mechanisms to enable shell growth

Trace elements present in seawater are incorporated within the shell structure of calcifying organisms and several empirical relationships have been observed between the trace element to calcium ratio and environmental parameters of the surrounding water. For example, the Mg/Ca ratio of a shell is positively correlated with the temperature of the surrounding water (Nürnberg et al. 1996, Dwyer et al. 2002, Pérez-Huerta et al. 2008, Kamenos et al. 2013). Based on empirical and experimental calibration, several element to calcium ratios have been observed to reflect the environmental condition. Trace element to calcium ratios and particularly Mg/Ca and Sr/Ca have been widely used to understand the biomineralisation process (but noted that biological activity can influence the elemental composition in the mineral rather than recording the environmental conditions, Weiner and Dove 2003). For example, OA has been shown to affect trace element to calcium ratios in corals (Sinclair 2005), foraminifera (Elderfield et al. 1996, Keul et al. 2013, Not et al. 2018), ostracods (Dwyer et al. 2013), and tubeworms (Chan et al. 2015b), but not sea urchins (Byrne et al 2014). For sea urchins grown under OA and

warming from the juvenile to the adult stage, the Mg/Ca was not affected by OA but, as expected, was altered by temperature (Byrne et al. 2014). When exposed to OA, Mg/Ca increased in vermetid shells, suggesting a dissolution of aragonite and increase in calcite (Chan et al. 2012, Milazzo et al. 2014). Milazzo et al. (2014) applied inductively coupled plasma optical emission spectrometry (ICP-OES) techniques to understand impacts of OA on calcification as growth and suggested that under OA shell dissolution will occur with the potential to impact survival through weakened shell protection.

Mass spectrometry

A variety of methods are available to measure the elemental ratios of a biological mineral. Basically, calcifying organisms can be measured in a solid phase using techniques such as X-ray fluorescence (XRF) or laser ablation (LA) or in dissolved phase after dilution using a range of inductively coupled plasma spectrometry. Since trace elements are measured within the mineral, several cleaning steps are required to remove organic matter and potential lithogenic contamination (Martin and Lea 2002). Typically, analysis of a dissolved sample by inductively coupled plasma (ICP) spectrometry requires the preparation of the shell or skeleton sample by acid digestion, fusion, or ash drying. Techniques for solution analyses include, ICP- optical emission spectrometry (OES), ICP- atomic emission spectroscopy (AES), ICP-mass spectrometry (MS), and multiple collector (MC) ICP-MS. The differences between these ICP spectrometry techniques are the increase of precision of the analyses, the higher resolution and therefore lower detection limits of elements up to isotopic measurement with MC-ICP-MS, whereas the disadvantages are the cost and maintenance of the equipment.

Electron microscopy AEM/ EDS/ SIMS/ EELS

Spatial information of elemental distribution in the mineral provides valuable information to predict mechanical properties. Solid-sampling methods have been developed for ICP analysis for this purpose. Electro-thermal-vaporisation (ETV) and laser ablation (LA) are applied to generate vapour for characterisation. In combination with ICP-OES or ICP-MS, these techniques are suitable for analysis of a solid sample (Limbeck et al. 2017). However, LA-ICP-MS only provides resolution of > 5 µm, while secondary ion mass spectrometry (SIMS) distinguishes sub-micrometre resolution (Becker et al. 2010). Although SIMS has a sensitive detection level of 1 ppm, the technique is not directly quantitative

due to its dependence on a solid-state chemical standard, and the nonlinear and highly variable nature of the ionisation process of different elements in SIMS (Williams 1985). In addition, SIMS can be used to obtain depth profiles of mineral composition of shells (Jeffree et al. 1995). All of these methods have an advantage of giving spatial information on the elemental distribution, the differences lie in the resolution between ICP-MS, ICP-OES and SIMS. ICP-OES is already applied using acid digestion of collected individuals for determination of elemental ratios (Milazzo et al. 2014). The application of SIMS to OA research would enable the analysis of much smaller samples and to examine the response of individual calcifying organisms in terms of growth and survival (Eichner et al. 2017).

The spatial detection of trace elements on a bulk material surface can be achieved through electron microscopy (Müller et al. 2011). Analytical electron microscopy (AEM) with energy dispersive X-ray spectrometry (EDS) and wavelength-dispersive X-ray spectroscopy (WDS) provides data at the nanometre scale (Newbury 1998). EDS offers an advantage of greater specimen area than the high resolution method of electron energy loss spectrometry (EELS), which also requires a 10 nm thick specimen to be prepared. Therefore, EDS is a more efficient and accessible AEM approach for OA research. Notably, detection levels of AEM-EDS are around 1000 ppm, EELS 10 ppm and structured illumination microscopy (SIMS) 1 ppm. EDS and WDS both enable the microanalysis of biominerals and provide additional spatial information of the elemental profile. The cost of EDS is considerably lower than WDS and has a high acquisition speed. In comparison, the spectral resolution of WDS is superior to that of EDS. These techniques have been applied to address the question of whether OA would have an impact on the calcification of shrimp and tubeworm skeletons, in order to understand the impact on exoskeleton critical function including protective defense against predators (Chan et al. 2012, Taylor et al. 2015). EDS was employed to determine magnesium content in the exoskeleton of shrimps grown under OA with the finding that increased calcium content with lowered pH resulted in a greater Mg/Ca ratio (Taylor et al. 2015). Mg/Ca as an environmental indicator of calcite has been suggested to increase as aragonite saturation decreases (Chan et al. 2012).

Taken together, there has been significant growth in a number of techniques available for quantifying elements present in liquid and solid materials. Some of the surface techniques such as LA-ICP-MS, and other analytical electron microscopy (AEM) techniques, such as SIMS, AEM-EDS and AEM-EELS,

415 have different resolutions and sample preparation requirements which should be considered in the
416 context of experimental objectives. The recent development of MS analytic methods for bioimaging
417 opens opportunities to investigate mineralising tissues at the biomolecule level (Becker et al. 2010).
418 Complementing optical and electron microscopy techniques as discussed in the following section, these
419 tools will enable a better understanding of the mechanism of OA impacts on the processes involved in
420 the production of biominerals. However, these techniques at present have the disadvantages of requiring
421 sample specific standards for calibration, time consuming sample preparation, observation confined to
422 a tiny area of interest and the destructive nature of sample analysis.
423

424 *Mineral composition analyses by FTIR and XRD*

425 Mineral composition characterisation techniques target the comparison of mineral phases, elemental
426 ratios and amorphous calcium carbonate to clarify the intricate process of biomineralisation (Figure 4).
427 In the context of OA, it is important to understand the process of biomineralisation mechanisms to
428 appreciate how continued growth will be possible under future environmental change.

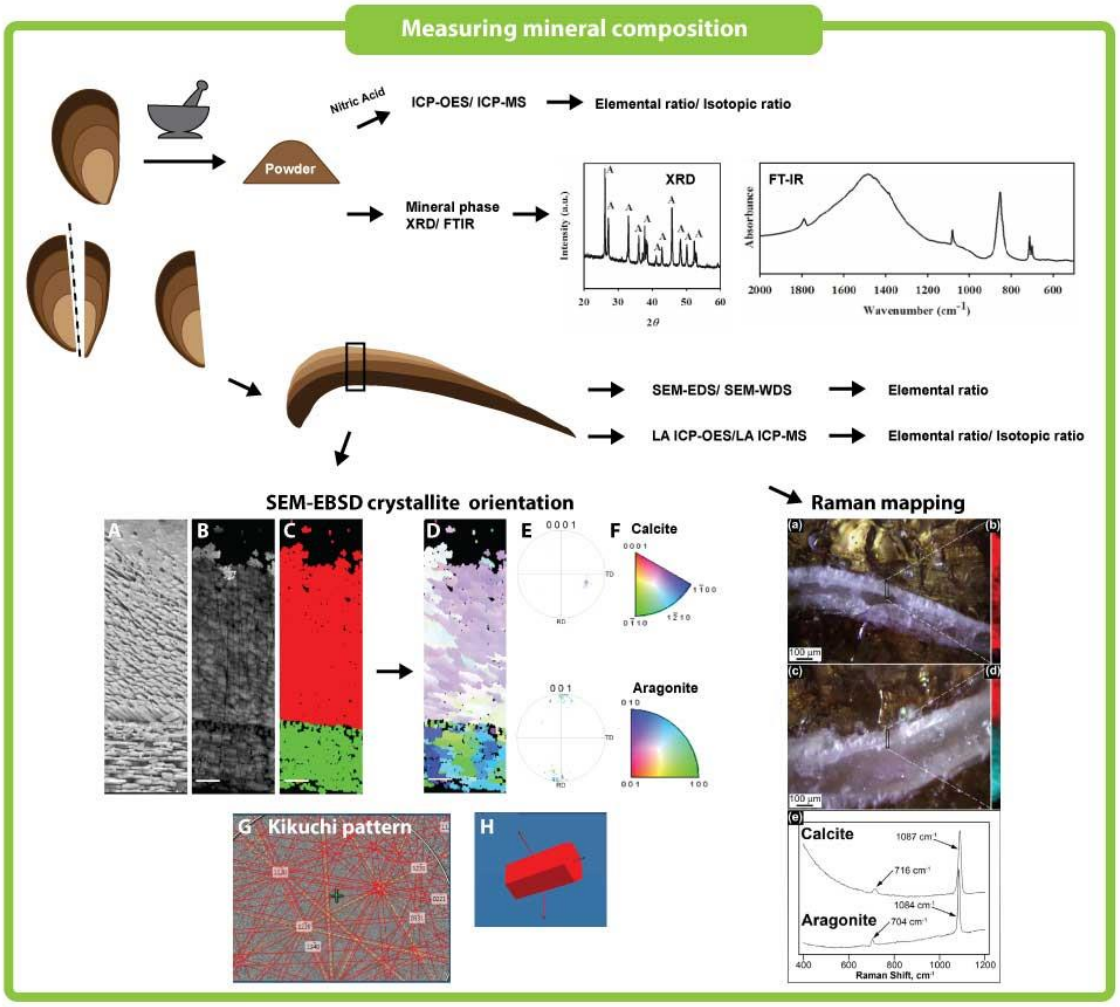

Figure 4. Schematic representation of highlighted techniques for characterizing mineral composition in biomineralising organisms. Shell power samples are digested prior to mass spectrometry characterisation, e.g. ICR-OES/ICP-MS, for determining elemental ratio or isotopic ratio. Sectional surface of the shell are inspected for elemental ratio mapping using electron microscopy techniques such as SEM-EDS or SEM-WDS; or using mass spectrometry approaches by LA-ICP-MS or LA-ICP-OES. Additionally, a sample of shell powder provides mineral phase indentification using FTIR or XRD, figures modified from Chan et al., (2012). SEM-EBSD, SEM-WDS and Raman spectroscopy are highlighted as techniques to determine the mineral composition and crystallographic orientation in a mussel shell to determine the impacts on shell growth under OA as an alternative to techniques such as ICP-OES or ICP-MS to determine elemental or isotope ratios in biominerals. SEM-EBSD figure

data taken from Fitzer et al., (2014a). Secondary electron images of the crystal structure from an etched (a) and polished (b) sample, the mineral composition can be seen in the phase map where calcite is shown in red and aragonite in green (c). The crystallographic orientation map (d), corresponding pole figures (e) and colour keys (f) are indicated for calcite and aragonite. EBSD uses Kikuchi patterns to identify the mineral phase (g) and the crystallographic orientation (h). Raman mapping figure modified from Chan et al., (2015b). Raman microscopy has been used to provide photomicrographs of younger (a) and older regions (c), of a juvenile tubeworm, phase maps indicate regions of aragonite only (b) and aragonite and calcite (d) in the tube. A Raman spectra (e) of aragonite and calcite has been measured in the same specimen (c).

Fourier-transform infrared (FTIR) spectra can be used to determine the relative quantity of amorphous calcium carbonate from an intensity ratio ($I_{max}\nu_2/I_{max}\nu_4$) between the absorption bands. The major disadvantage of the FTIR approach is its semi-quantitative nature; results can only be compared within the same experimental dataset. This method has been adopted in OA research on a marine tube worm where amorphous calcium carbonate content was found to be higher at low pH (Chan et al. 2012, Leung et al. 2017). Chan et al. (2012) suggest that this result indicates the presence of an active shell repair mechanism when animals are counteracting shell weakening by OA. The advantage of FTIR is that it takes as little as 1 mg of mineral sample and so may be applied to larval specimens.

The ratio of calcite and aragonite content, that has implications for the vulnerability of shells and skeletons to OA, can be quantified by X-ray diffraction (XRD). This is an advantage over FTIR, but XRD has its own drawback, i.e. the loss of spatial resolution due to the need for powdered samples. XRD approach has been used to assess shell or exoskeleton growth under OA. Unless containing large amounts of Mg, calcite is considered to be less susceptible to dissolution at lower pH values than aragonite (Ries et al. 2009, Chan et al. 2012). OA relevant changes in thickness of the calcite and aragonite layers was first noted in mussels transplanted into low-pH environments (Hahn et al. 2012). Calcite: aragonite ratios have been shown to change under OA, leading to a thinner and more vulnerable

aragonite layer in mussel shells (Fitzer et al. 2015a). The shell thickness index in comparison to the measured thickness of the aragonite or calcite layers uses the thickness, the length, height and dry mass of the shell and is considered to produce a lower measurement error compared to direct measurement (Freeman and Byers 2006, Naddafi and Rudstam 2014, Fitzer et al. 2015a). The shell thickness index, in comparison to XRD, has an advantage of being non-destructuive to the sample, but a disavantage with a loss in spatial resolution.

Raman spectroscopy

Raman spectroscopy is a non-destructive technique that enables molecular bonds and mineralogical information to be precisely characterised at a submicron resolution. By illuminating a sample with a monochromatic laser beam, a Raman spectrum is generated that contains unique peaks that are diagnostic of mineral polymorphs due to their characteristic Raman shifts (Eisenstein et al. 2016). Structural components, such as calcite, aragonite and collagen, have been identified and mapped with resolution as fine as 1 µm (Eisenstein et al. 2016, Taylor et al. 2016). Advantages of Raman spectroscopy over other spectroscopic methods, such as FTIR, include the improved spatial resolution and the direct relevance of this method for biomineralisation, as well as the potential to examine samples in their native state (Eisenstein et al. 2016, Von Euw et al. 2017). This technique is considered a complementary method to FTIR, and is perhaps more suitable for OA studies. Raman microscope imaging has been applied to OA research to identify the mineral composition and polymorphic forms to assess rates of calcification under increasing pCO_2 in coralline algae and limpets (Kamenos et al. 2013, Langer et al. 2014). For instance, Raman mapping of the shells of limpets from a CO_2 vent demonstrated that the polymorph distribution pattern is maintained despite living at low pH (Langer et al. 2014). In coralline algae, although calcification continues under OA, Raman has identified disorder in the molecular position of the carbonate ions which suggests a weakened skeletal structure (Kamenos et al. 2013). These applications were used to assess exoskeleton structural weaknesses which can impact the protective function of the calcified structures under OA.

SEM-EBSD

Electron backscatter diffraction (EBSD) is widely used to determine the crystallographic orientation of biogenic minerals. EBSD provides additional information to precursory SEM imaging of shell dissolution or exoskeletal microstructure as it allows for the examination of microstructure at the individual crystal level. The technique identifies Kikuchi patterns (Kikuchi 1928, Nishikawa and Kikuchi 1928) as scattered electrons are reflected as per Bragg's law from the crystal lattice onto a phosphorus screen. It was first used to observe the impact of OA on the shell ultrastructure of the mussel *Mytilus galloprovincialis* (Hahn et al. 2012) and was further applied across a broad range of species, including an argonaut (Wolfe et al. 2013) and corals (Fitzer et al., 2014b; Hennige et al., 2015). The effects on crystalline structure identified using this technique in OA research have been used to address the question of how changes in seawater environment can impact the orderly arrangement of shell or exoskeleton structures which has an implication to the animal's ability to survive.

X-ray microscopy XPEEM – XAS and XANES

An alternative emerging technique for determining the mineral composition of marine skeletons is high-spatial resolution synchrotron X-ray photo emission electron microscopy (XPEEM) combined with X-ray absorption spectroscopy (XAS) (Fitzer et al. 2016). The benefits of the XPEEM and XAS over SEM is the high level of spatial resolution, and the fact that it can detect without the need for an energy filter by measuring the secondary electrons yield as a function of photon energy. This technique can be applied alongside electron backscatter diffraction (EBSD) to identify mineral phases throughout the shell structure (Fitzer et al. 2016). XANES and XPEEM techniques use the principles of X-ray absorption fine structure (XAFS) which interpret the scattering of photo-electrons emitted from an absorbing atom in a structure when excited by high energy photons (Politi et al. 2008, Fitzer et al. 2016). XANES has been used as a tool to examine the phase transformation mechanisms of amorphous calcium carbonate into calcite particularly in sea urchin larval spicules (Politi et al. 2006, Politi et al. 2008, Gong et al. 2012). Recently, XPEEM combined with XAS has been used as a tool to examine amorphous calcium carbonate in mussels reared under OA conditions (Fitzer et al. 2016) showing more induced amorphous calcium carbonate with less crystallographic control over shell formation. This technique

519 was applied to address the question of OA impact on biomineralisation and shell repair to determine
520 the protective function of the shell under changing environments (Fitzer et al. 2016). The technique
521 requires the embedding and fine-polishing of samples, similar to SEM-EBSD preparation (Politi et al.
522 2008, Perez-Huerta and Cusack 2009, Fitzer et al. 2016). XANES and XPEEM have the advantage of
523 providing high spatial resolution to locate amorphous calcium carbonate embedded within the shell
524 structure when applied in combination with SEM techniques (Politi et al. 2008). Disadvantages include
525 the high instrumentation cost and lengthy sample preparation time.

526 *AFM*

527 Atomic force microscopy (AFM) provides atomic resolution analysis of material properties. As a type
528 of scanning probe microscopy, AFM scans and interacts with a sample directly using a tip that is
529 connected to a cantilever spring. The vertical deflection and the force-distance curve are recorded by a
530 piezoelectric translator (Butt et al. 2005). In tapping mode, AFM generates fine topographical images
531 with nanometre resolution. The time-dependent relationship between applied pressure (stress) and
532 deformation (strain) represents viscoelastic properties (Butt et al. 1995) enabling the measurement of
533 local mechanical properties.

534 Easy sample preparation and high resolution are the major advantages of using AFM over conventional
535 microscopy methods (Butt et al. 1995). The typically small interacting surface for AFM must be smooth
536 and homogeneous requiring polished and etched surfaces similar to EBSD sample preparation (Dalbeck
537 et al. 2011). Therefore, AFM complements the observations of SEM-EBSD analysis which can provide
538 high resolution textural data to OA studies (Dalbeck et al. 2011). AFM performed in the presence of an
539 electrolyte solution is possible (Butt et al. 1995), therefore, enabling better biological relevance. In order
540 to obtain comparable regions of interest, correlative SEM or light microscopy data are often helpful to
541 effectively navigate at AFM resolution (Sikes et al. 2000). AFM has yet to be applied to determine the
542 impact of OA on biomineralisation. Once applied, this technique will provide a correlation with EBSD
543 data to address the question of biomineralisation mechanisms in shell growth and hence survival.

544 *FIB-TEM*

The finest biological observation have been via transmission electron microscopy (TEM), providing resolutions of nanometres down to below an ångström (Nellist et al. 2004) exceeding 'super-resolution' microscopy. In addition, TEM is an important characterisation tool that collects X-ray diffraction with a micrograph enabling subcellular features and location of crystals to be analysed together. A nanofabrication technique using the focused ion beam (FIB) system has emerged as a powerful tool for precise TEM specimen preparation, where milling and cutting of a sample is performed inside an SEM or scanning ion microscopy (SIM) (Titze and Genoud 2016). This preparation approach overcomes technical challenges of manual preparation of ultrathin TEM sections, with the localisation of the region of interest, and reduces the risks of sample loss (Chan et al. 2017).

Suzuki et al. (2011) revealed the details of five microstructures in the limpet shell using FIB-TEM. The FIB technique was used to separate each microstructure in cross section to determine crystal morphology and orientation. The FIB technique is powerful in handling tiny larval or juvenile shells (Yokoo et al. 2011, Chan et al. 2015a, Chan et al. 2017), and reduces costs of analysis time for TEM on samples with poor orientation or an unfocussed area of interest. FIB-TEM ensures a consistent cutting angle at the nanoscale, so providing comparable observation of a larger number of experimental samples.

Depending on institutional resources, fine spatial resolution, long-hour procedures performed using FIB-TEM can be costly in a centralised facility. In summary, FIB-TEM is currently a qualitative observational method, but it has potential to be applied in a more quantitative setting.

Cryo-electron microscopy

In cryo-electron microscopy, biological samples can be visualised by a freeze fracture process which is achieved by rapid freezing of fixed tissue samples by vitrification (Alfredsson 2005). A hydrated sample that is close to the native state can be observed in high resolution without the requirement of destructive conventional preparation procedures for SEM and TEM (Levi-Kalisman et al. 2001, Khalifa et al. 2016, Thompson et al. 2016). Electron microscopy also enables X-ray diffraction characterisation essential for identification of minerals. Ice from humidity in the environment can contaminate the sample,

571 therefore, samples must be prepared after vitrification (Thompson et al. 2016). Technical disadvantages
572 associated with cryo- methods include the need for stabilising detergents for structure (Singh and
573 Sigworth 2015) which, in addition to its high cost, will make the application of this technique
574 challenging for large scale OA experiments.

575 *Stable isotopes*

576 Biogenic stable isotopes have been used extensively to reconstruct the paleaoclimates, in terms of
577 temperature, pH and salinity (Lear et al. 2000, Parkinson et al. 2005, Ghosh et al. 2006, McConnaughey
578 and Gillikin 2008, Martin et al. 2016, Stewart et al. 2016). They can also be used to understand
579 biomineralisation mechanisms of ion transport at the site of calcification (Furla et al. 2000, Rae et al.
580 2011, Allen et al. 2012, Allison et al. 2014). The detection of Mg, Sr, and Ca, the detection of the
581 isotopes, $\delta^{13}C$, $\delta^{18}O$, ^{10}B and $\delta^{11}B$ requires acid digestion prior to mass spectrometry analyses (Krief et
582 al. 2010). Here, we list some of the target isotopes that have promise for OA research.

583 Quantification of isotopic elements can be applied to detect the consequence of stress on calcification
584 pathways (Rae et al. 2011, Allison et al. 2014, Stewart et al. 2016). Brachiopods, in particular, form
585 their exoskeletons in good isotopic equilibrium with the seawater (Parkinson et al. 2005). Since pH is
586 dependent on two boron species: boric acid ($B(OH)_3$) and the borate ion ($B(OH)_4^-$) (Hemming and
587 Hanson 1992, Stewart et al. 2016, Zhang et al. 2017), the species of boron isotopes found in shells
588 represents the dissolved inorganic carbon (DIC) chemistry of the calcification fluid (Allison et al. 2014).
589 Stable isotope techniques have been applied in OA research to understand the mechanisms of
590 biomineralisation, specifically, whether material is laid down under control by the organism irrespective
591 of the seawater isotopes (Krief et al. 2010). For example, seawater pH impacts the skeletal $\delta^{13}C$ and δ
592 ^{18}O in corals, but there is an offset in the $\delta^{11}B$ between the calcified material and that of seawater
593 suggesting control of biomineralisation by ion-transport enzymes (Krief et al. 2010). This technique
594 addresses the question of calcification mechanism change under OA and whether there is a reduced
595 metabolic incorporation of isotopes through enzyme control, hence reduced growth and survival under
596 OA. The influence of carbonate ion concentration on $\delta^{13}C$ and $\delta^{18}O$ is still being explored, particularly
597 in foraminifera (Spero et al. 1997).

598 Isotopic approaches have the disadvantage of requiring a relatively large amount (~2 mg) of biogenic
599 calcium carbonate powder. Sample preparation with micro-milling is time-consuming and can be
600 technically challenging, especially when investigating different polymorphs and seasonal growth bands
601 in smaller specimens (Stewart et al. 2016). Advances in stable isotope techniques will consist of
602 improved ways of separating organics from biominerals, micro milling samples for biomineral powder,
603 and laser ablation methods that increase spatial resolution of measurements (Fietzke et al. 2010, Wall
604 et al. 2016).

605 *Radioactive isotopes*

606 In addition to using ^{45}Ca for estimation of calcification, radioactive isotopes can also contribute to a
607 mechanistic understanding of the calcification process. Furla et al. (2000) used a double radioactive
608 isotope experimental design ($H^{14}CO_3$ and ^{45}Ca) to show inorganic carbon transport. Comprehensive
609 measurement of both the DIC species and Ca for calcification was accomplished in terms of net
610 radioactivity by ^{14}Ca and ^{45}Ca (Furla et al. 2000). These data also unraveled the carbonate concentrating
611 mechanisms within coral cells (Furla et al. 2000).

612 The use of radioactive isotopes (^{45}Ca, ^{14}C) is specific and sensitive to experimental conditions.
613 Moreover, the maintenance of radioactive substances can be challenging. Before adopting the use of
614 radioactive isotopes within an experimental culture, a protocol must be optimised to adequately label
615 specimens and avoid contamination. Therefore, even though the approach is quite well-established in
616 environmental geochemistry (Parkinson et al. 2005, Ghosh et al. 2006, McConnaughey and Gillikin
617 2008), disadvantages of requiring continual radioactive tracer application and the destructive nature of
618 the sample digestion by acid means that it has yet to be applied more widely in OA studies (Furla et al.
619 2000).

620 **Cellular biomineralisation mechanisms**

621 The processes by which organisms control the substrate for calcification are complex and can occur
622 internally within tissues, or outside the organism, but both need to modify the seawater chemistry for
623 calcification to take place (Roleda et al. 2012). It is thought that HCO_3^- is the choice of substrate for

biomineralisation, which can be taken directly from seawater or metabolised from CO_2 (Roleda et al. 2012). The mechanisms revolve around producing an abundance of ions and the right conditions to favour the precipitation of $CaCO_3$ from available Ca^{2+} and CO_3^{2-} (Roleda et al. 2012). An understanding of biomineralisation mechanisms under forecasted OA conditions will require the use of a wide range of techniques (Figure 5) but also working at different levels, from genes to organisms and ecosystems. This can be achieved by taking advantage of established techniques from other disciplines. For example, methods to culture larval sea urchin primary mesenchyme cells facilitates the study of the calcification process *in vitro* (Basse et al. 2015). Identifying and evaluating the roles of organic molecules in shells is a major topic in biomineralisation as the mechanical properties of shells are highly influenced by their 1% content of organic components. In the context of OA impacts on marine calcifiers, the response of organic molecules provides an insight into cellular mechanisms for the ability to reproduce and develop and can be applied to all marine organisms irrespective of size (Figure 1, schematic of question vs scale). Mechanisms of biomineralisation are largely unresolved and vary from species to species.

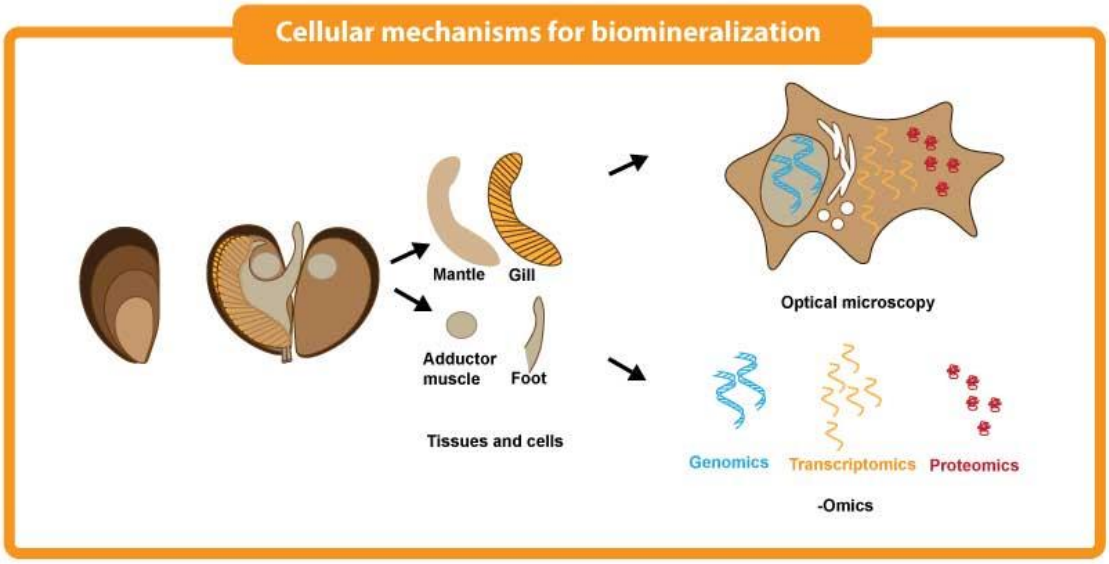

Figure 5. Schematic representation of techniques to examine the cellular mechanism of biomineralisation. Techniques with OMICS, optical microscopy are established techniques that could be applied on various tissues and cells to determine the impact of OA on molecular biomineralisation.

642

643 *SDS-PAGE and MS*

644 Shell protein extraction is achieved by recovering the protein from decalcified shell. Sodium dodecyl
645 sulfate-polyacrylamide gel electrophoresis (SDS-PAGE), or 2D gel electrophoresis enables a
646 comparison of protein profiles. In addition, mass spectrometry (MS) also enables the identification of
647 proteins from available databases. As marine organisms studied in OA research are usually not 'model-
648 organisms', protein identification is challenging. Protein purification, protein sequencing, and protein
649 digestion, may be required in the identification process (Marxen et al. 2003, Suzuki et al. 2004). When
650 a large protein (more than 30 kDa) needs to be identified, cloning methods can be used to recover the
651 nucleotide sequence for deduction of the protein sequence (Miyamoto et al. 1996, Samata et al. 1999,
652 Suzuki et al. 2009, Suzuki et al. 2011). Many genome and transcriptome databases of calcifying
653 invertebrates generated by next generation sequencing are also available as open resources (Takeuchi
654 et al. 2012, Zhang et al. 2012).

655 MS is also a promising technique to understand shell proteins. The MS/MS spectra of peptides allow
656 determination of amino acid sequence without the need for a protein sequencer and has become a low
657 cost and high throughput technique. The combination of MS/MS and databases from next generation
658 sequencing is dramatically increasing the efficiency of protein identification (Joubert et al. 2010,
659 Marie et al. 2010, Marie et al. 2011). The potential disadvantage of generating big data from the high
660 throughput process is covered in more detail in the next Section. These techniques have been applied
661 to show the proteome responses of invertebrates grown in OA conditions. For example, the shell
662 matrix proteins of the larval pacific oyster (*Magallana gigas*) were observed to decrease under OA
663 (Harney et al. 2016).

664 SDS-PAGE and MS offer advantages of low cost and in the case of MS high throughput protein
665 identification to understand why physiological responses may be influenced by ocean acidification.
666 The disadvantages of these techniques include time-consuming sample preparation to extract and
667 purify proteins for analysis and production of big data which can be difficult to interpret.

Insoluble organic component analyses using XRD, IR and pyrolysis NMR, and dyes

Insoluble organic components in the shell, such as chitin, are an essential polysaccharide that connects organic matrices and the initial deposition of the mineral (Nakayama et al. 2013); it serves as a scaffold for organic materials during the deposition of minerals. For example, the molluscan periostracum is made of chitin and it serves as a waterproof layer of a calcification compartment. Chitin is commonly found in the forms of α and β-chitin. Crustaceans use α-chitin in their exoskeletons and molluscs use β-chitin in their shells, as such, chitin is an essential additive to greatly improve the mechanical properties of biomaterials. Due to the insoluble and organic nature of chitin, the impact of OA on chitin content is currently unknown. There are many techniques to identify chitin, including X-ray diffraction (Weiner and Traub 1980, Levi-Kalisman et al. 2001, Falini et al. 2003), infra-red (IR) spectroscopy in the finger printing region (700-1800 cm^{-1}) (Pearson et al. 1960), and nuclear magnetic resonance (NMR) or MS detection of the glucosamine hydrochloride after hydrolysis (Nakayama et al. 2013). The analysis of pyrolysis (thermal decomposition of materials in a vacuum) GC-MS is able to identify characteristic chitin decomposition markers (Furuhashi et al. 2009). However, many other contaminants (such as proteins) produce a complex of unknown peaks that make the identification of chitin in biominerals difficult and, in the case of insufficient crystallinity, a clear diffraction pattern may be hard to obtain. Recently, a colorimetric assay of chitin has been developed to quantify chitin (Katano et al. 2016). The workers found that upon complete hydrolysis of chitin in strong acid (5M HCl), characterization of depolymerized glucosamine is possible using colorimetry at the absorbance maximum at 750 nm. The method requires small amount of sample (10 mg), it is low cost, simple and quantitative. However, the detection is robust and cannot distinguish polymorphs and spatial distribution of chitin.

Chitin can be visualised microscopically by calcofluor white which binds strongly to cellulose and chitin, and wheat-germ agglutinin (WGA) which binds to N-acetyl-D-glucosamine and sialic acid (Suzuki et al. 2007). Due to the non-specific nature of calcofluor-white and WGA, more specific detection is accomplished by using chitin-binding domain fused with green fluorescent protein (CBD-GFP) as shown in the larval shell of *Mytilus galloprovincialis* (Weiss and Schönitzer 2006) and the

prismatic layer of *Atrina rigida* (Nudelman et al. 2007). Quantifying the expression of the chitin synthase gene is an alternative approach to measure chitin production (Cummings et al. 2011).

While the role of chitin may be essential in providing a waterproof cover and biomineralisation framework to the shell formation process, the plasticity of chitin synthesis under OA environmental stress has not yet been investigated. Chitin has many important biological roles in a diverse taxonomic group of animal models (Lee et al. 2011), therefore, the detection of chitin could provide valuable information on both the structural and functional responses to OA. The disadvantages of XRD, IR, and pyrolysis NMR or GC-MS techniques for chitin analysis such as the low abundance of organic materials in calcareous structures and therefore time-consuming sample preparation may limit the application of this approach to future OA studies. On the other hand, visualizing chitin with dyes such as calcofluor white and WGA are prone to non-specific reactivity to other molecules than chitin. The more specific CBD-GFP labeling requires bioengineering protocol to express and purify the chitin probe.

OMICS

Omics studies are generating "big data". However, these data cannot be simply used as proxies of fitness (Feder and Walser 2005). As a consequence, little information can be extracted from purely exploratory studies (e.g. comparisons between two OA scenarios). A more powerful approach involves the analysis of the data to test a hypothesis based on physiological or ecological experiments. For example, De Wit et al. (2016) filtered a large-scale transcriptomic database to select genes following the same pattern identified at the physiological level in copepods exposed to OA (Thor and Dupont 2015, De Wit et al. 2016). The future use of omics to investigate the effects of OA on biomineralisation is promising, especially using the integration of omics technique with other physiological endpoints.

The three main omics approaches to consider are transcriptomics, proteomics and metabolomics. Transcriptomics is a study of mRNA and actively expressed genes, while proteomics investigates the total protein profile, and metabolomics capture the biochemical status of an organism.

Transcriptomic changes can provide insights into genetic pathways involved in calcification by comparison of gene expression, for example at different stages of calcification, or under different

720 environmental conditions. That is, when applied in a time series, changes in transcriptomes of
721 developing larvae provide useful information relevant to the onset of biomineralisation (Zhang et al.
722 2012). De Wit et al. (2018) used OA as a tool to delay calcification in early stage of oyster development
723 and using a time series were able to identify genes involved in larval shell calcification (De Wit et al.
724 2018). Under OA, transcriptomic studies are used to assess the physiological capacity of organisms by
725 studying not just the biomineralisation molecular pathways but also the other related pathways giving
726 a complete picture in understanding the consequences of living in a high CO_2 oceans (Todgham and
727 Hofmann 2009).

728 Proteomics investigates the total protein profile. Since proteins are the active functional units of an
729 expressed gene, these data are closer to the organism at the functional level and phenotype. Proteomes
730 can be altered by OA, as shown by different calcification protein expression in oysters (Dineshram et
731 al. 2015). The organic matrix proteins that are associated to shell deposition have been profiled in corals
732 (Drake et al. 2013), oysters (Suzuki and Nagasawa 2013), and blue mussels (Suzuki et al. 2011),
733 although this information has not been profiled in the OA context.

734 In common with the transcriptome, some precautions should be taken during the interpretation of a
735 proteome. The quantity of a protein commonly cannot be directly linked to the fitness of an organism
736 as regulatory post-translational modifications play a key role (Mann and Jensen 2003). This is an
737 essential consideration for the study of shell proteins which are often heavily glycosylated,
738 phosphorylated or tyrosine sulfated as required for calcium binding (Zhang and Zhang 2006).

739 A major disadvantage of applying OMICS to the study of biomineralisation is the low abundance of
740 about 5% organic content in calcareous structures (Zhang and Zhang 2006). In order to isolate sufficient
741 protein or polysaccharide for analysis, a large amount of shell must be used. In addition, the extraction
742 and purification of the organic content is greatly influenced by decalcification, and the shell can often
743 contain organic impurities (Watabe 1965). Researchers should be aware of technical limitations using
744 different characterisation techniques, for example 2D gels have a lower sensitivity than iTRAQ analysis
745 (Wiese et al. 2007). In addition, the interpretation of OMICS data is highly dependent on genomic
746 information, therefore, it remains as a challenging method for non-model organisms.

Cellular pH imaging

When live imaging is conducted, inverted microscopy enables living marine organisms to be fully submersed in seawater during observation (Venn et al. 2011, Stumpp et al. 2012, Tambutté et al. 2015, Chan et al. 2017). In some imaging methods, synthetic ratiometric images are generated by sequential images of the same region of interest. Mobile organisms can be immobilized (e.g. 2-4% agarose seawater or using micropipettes) to enable image acquisition of the region of interest. For longer periods of observation, a perfusion chamber is necessary to remove metabolic waste and allow exchange of aerated experimental seawater with enriched CO_2.

Fluorescent microscopy has been applied to visualise the calcification compartment during mineralisation at a low seawater pH using markers including calcein, alizarin and calcofuor white for *in situ* analysis of calcification and tracking of calcification as shown for coralline algae (Lewis and Diaz-Pulido 2017). Newly deposited minerals can be quantified from their fluorescent appearance at their respective excitation (Exλ) and emission wavelengths (Emλ), e.g. alizarin: Exλ = 530-560 nm, Emλ = 580 nm; calcein: Exλ = 494 nm, Emλ = 517 nm; calcofluor white: Exλ = 365 nm, Emλ = 435 nm. Calcein is a preferable marker because of its high efficiency, non-invasiveness (Lewis and Diaz-Pulido 2017) and it is relatively low in cost. In addition, the fluorescent region can be isolated and characterised using the techniques described for measuring growth and development in the earlier sections .

The heterogenous distribution of carbon sources, e.g. CO_3^{2-} ions at the calcification site, can be monitored by measuring intracellular pH (de Nooijer et al. 2008, Venn et al. 2011, Venn et al. 2013, Tambutté et al. 2015). Similar to the carbonate dynamics in the ocean, a shift in pH influences the DIC abundance in the biomineralisation compartment, in terms of CO_3^{2-} and HCO_3^-. As shown in foraminifera, pH of the site of calcification increases during calcification, while the surrounding ambient pH decreases probably through active proton pumping (Toyofuku et al. 2017). A higher pH value facilitates the conversion of CO_2 and HCO_3^- to CO_3^{2-} (Toyofuku et al. 2017), and both the CO_3^{2-} concentration and calcium carbonate saturation state can then be calculated (Venn et al. 2011, Venn et al. 2013, Tambutté et al. 2015). Furthermore, it is possible to estimate the amount of emitted proton by

774 image processing of pH sensitive ratiometric microsopy. Ratiometric fluorescent dyes enable the
775 monitoring of intracellular and extracellular pH (Chan et al. 2015a, Comeau et al. 2017b, Toyofuku et
776 al. 2017). Several pH sensitive dyes are available depending on the tested pH range. When the cell
777 permeable dye SNARF-1 acetoxymethyl ester is excited at a wavelength of 543 nm, the ratio of
778 fluorescence captured at emission wavelengths of 585 ± 10 nm and 640 ± 10 nm shows a linear
779 relationship to intracellular pH (Venn et al. 2013). Similarly, cell impermeable SNARF-1 can be used
780 to measure pH in the calcifying fluid in corals; 2'-7'-bis(carboxyethyl)-5(6)-carboxyfluorescein
781 (BCECF) for intracellular pH of echinoderm larvae (Stumpp et al. 2012) and pyranine for foraminifera
782 (Toyofuku et al. 2017). This technique has been applied to OA to investigate how growth and
783 calcification rates are impacted by increasing pCO_2 (Stumpp et al. 2012), where extracellular pH was
784 actively compensated.

785 More recently, measurement of intracellular pH employs the use of microelectrodes between 10 and 15
786 µm tip diameter for direct in-tissue measurement (Cai et al. 2016), using pH polymeric membrane
787 microelectrodes (Zhao and Cai 1999), and CO_3^{2-} electrodes (Cai et al. 2016). Using this approach, pH
788 and CO_3^{2-} were observed to sharply increase in the calcifying fluid of various coral species, confirming
789 the presence of H^+ pump (Cai et al. 2016). In addition to intracellular pH determination, microelectrodes
790 can be designed to monitor dissolved oxygen and calcium concentration to enable analysis of a wider
791 range of parameters (Glas et al. 2012a, Glas et al. 2012b). The cellular pH imaging techniques have an
792 advantage of high spatial resolution for direct in-tissue measurement, however, the disadvantages
793 include time consuming sample preparation. This includes the challenge that organism immobilization
794 strategies varies and the protocol requires optimization to ensure the organism is capable of generating
795 biominerals. Ratiometric pH probe also requires calibration before the ratios can be converted to pH
796 values.

797 *Physiological inhibitors and stimulators*

798 The use of physiological inhibitors or stimulators is a useful approach to investigate the biochemical
799 pathways and pumps involved with biomineralisation (Basse et al. 2015). How biological pathways
800 may be influenced by specific inhibitors can explain the mechanism of shell formation under OA

conditions. For example, treatment with adenylyl cyclase inhibitors alleviate the negative effects of OA in Pacific oysters, suggesting the potential mechanism change under OA (Wang et al. 2017). This result confirmed the role of adenosine triphosphate (ATP) generation is essential to support shell production (Pan et al. 2015). Not requiring complete genetic information is greatest advantage of using inhibitors and stimulators to evaluate the mechanisms of biomineralization in a reductionist approach (Toyofuku et al. 2017). However, the choice of inhibitors may be non-specific to a single pathway and its action requies verification by a known physiological end-point.

Combining techniques

The described techniques can be employed individually to answer specific scientific questions to determine the impact of OA on marine biomineralisation. However, it is important to consider combining techniques to address complex scientific questions.

Combining x-ray microscopy techniques

Due to the development of optimum sample preparation for the analysis of a flat surface (Perez-Huerta and Cusack 2009), the output of XPEEM with XAS (Fitzer et al. 2016) and SEM-EBSD (Hahn et al. 2012, Wolfe et al. 2013, Fitzer et al. 2014a, Fitzer et al. 2014b) can be readily compared. This has allowed the influence of OA on both the biomineral structure and composition to be determined for corals (Rodolfo-Metalpa et al. 2011), sea urchins (Bray et al. 2014), and mussels (Melzner et al. 2011). Likewise, the simple mapping of calcite and aragonite is applicable across a wide variety of species including mussels and limpets (Hahn et al. 2012, Langer et al. 2014, Fitzer et al. 2015a). In contrast, comparison of mineral composition between high-resolution microscopy with spectral techniques such as XRD, FT-IR, and XPEEM with XAS is more complex. The use of SEM imaging, and calcite and aragonite thickness by EBSD, or species-specific visual inspection using compound microscopy (Fitzer et al. 2014b), have their merits to examine larger areas of shell erosion. However, to examine the intricate details of biomineralisation and potential changes under OA conditions these methods should be used in conjunction with XRD, FT-IR, XPEEM with XAS, and SEM-EBSD.

Multi-omics data integration

827 Several -omics approaches can be integrated, i.e. multi-omics (Huang et al. 2017). For example, the
828 mantle transcriptome and shell proteomes were integrated to study the shell formation of the pearl oyster
829 (Joubert et al. 2010, Berland et al. 2011), enabling proteomics data to be analysed without a complete
830 genome. Similarly, proteomics and metabolomics were studied together in oysters (Wei et al. 2015). A
831 more complex multi-omics study examined the genome, transcriptome and proteome in the Pacific
832 oyster (Zhang et al. 2012). Such a multi-omics approach also provided insights on the phosphate
833 biomineralisation in brachiopods (Luo et al. 2015). This is a promising approach in the context of OA
834 to understand the fitness or survival of organisms.

835 **Conclusions: What now for OA research on biomineralisation?**

836 A range of tools are shown in this article to help researchers to determine the impact of OA on
837 biomineralisation mechanisms at physiological and molecular levels, and thus on shell or skeleton
838 structural mechanics. The purpose of this review is to discuss commonly available biomineralisation
839 tools for understanding this one physiological response to ocean acidification. However, organisms
840 have a complex physiological profiles, and it is important to note that biomineralisation is not an isolated
841 process, and not is it the only physiological process that needs to be considered in this context. Given
842 the nature of biomineralisation mechanisms and their complex responses to OA, a variety of
843 physiological, materials science, and crystallography tools are needed to thoroughly understand the
844 biomineralisation process and its vulnerability to OA. This review outlines techniques that can be used
845 to characterise, quantify and monitor the process of biomineralisation in a variety of calcifying marine
846 organisms, especially when they are cultured under OA experimental conditions. It also highlights basic
847 principles and the advantages and disadvantages of established, emerging and future techniques for OA
848 researchers. The key to developing a strategy aimed at better understanding the potential consequences
849 of OA is to define clear questions and hypotheses for testing. This would naturally lead to constrains
850 (e.g. tested species, quantity of material available, size) that, when combined with practicalities (e.g.
851 budget, equipment), will lead to selection of the appropriate experimental approach.

852 Recently, more attention has been paid to the underlying biological and physiological mechanisms of
853 biomineralisation. For example, tissues and external organic layers can protect the shell from corrosion

in under-saturated waters (Rodolfo-Metalpa et al. 2011). To address the underlying mechanisms affected by the impacts by OA, various methods need to be combined. For instance, determination of amorphous calcium carbonate is important to characterise mineral choice and relate phase transitions at the earliest stage of biomineral formation. Mechanisms of cellular involvement and specific biomolecules for biomineralisation can be examined using fluorescent microscopy and omics. The interactions of proteins in the extrapallial fluid and shell interface can be understood by applying techniques in isotope labelling and microscopy. It is also crucial to consider the fitness consequences of observed changes. For example, in a prey species, shell strength should be considered in relation to predator behaviour. The combination of established, emerging and future techniques will enable a holistic approach and better understanding of the potential impact of OA on biomineralisation by marine species and consequences for marine calcifiers and associated ecosystems.

Acknowledgement

The authors thank Andrew Mount, P. S. Murphy, Howard Browman and Kaimin Shih for their initial thoughts and input to this review at the 2nd Interdisciplinary Symposium on Ocean Acidification and Climate Change (ISOACC) meeting in Hong Kong December 2016. We also appreciate Sylvie Stambutte and Alexander Venn for their comments and suggestions to this review.

References

Addadi, L., Raz, S., and Weiner, S. 2003. Taking advantage of disorder: Amorphous calcium carbonate and its roles in biomineralization. *Advanced Materials* **15**:959-970.

Alfredsson, V. 2005. Cryo-TEM studies of DNA and DNA–lipid structures. *Current Opinion in Colloid & Interface Science* **10**:269-273.

Allen, K.A., Hönisch, B., Eggins, S.M., and Rosenthal, Y. 2012. Environmental controls on B/Ca in calcite tests of the tropical planktic foraminifer species *Globigerinoides ruber* and *Globigerinoides sacculifer*. *Earth and Planetary Science Letters* **351–352**:270-280.

Allison, N., Cohen, I., Finch, A.A., Erez, J., and Tudhope, A.W. 2014. Corals concentrate dissolved inorganic carbon to facilitate calcification. *Nature Communications* **5**:5741.

880 Anstis, G., Chantikul, P., Lawn, B.R., and Marshall, D. 1981. A critical evaluation of indentation
881 techniques for measuring fracture toughness: I, direct crack measurements. *Journal of the*
882 *American Ceramic Society* **64**:533-538.
883 Asnaghi, V., Chiantore, M., Mangialajo, L., Gazeau, F., Francour, P., Alliouane, S., and Gattuso, J.P.
884 2013. Cascading effects of ocean acidification in a rocky subtidal community. *PLOS ONE*
885 **8**:e61978
886 Basse, W.C., Gutowska, M.A., Findeisen, U., Stumpp, M., Dupont, S., Jackson, D.J., Himmerkus, N.,
887 Melzner, F., and Bleich, M. 2015. A sea urchin Na+K+2Cl− cotransporter is involved in the
888 maintenance of calcification-relevant cytoplasmic cords in *Strongylocentrotus droebachiensis*
889 larvae. *Comparative Biochemistry and Physiology Part A: Molecular & Integrative*
890 *Physiology* **187**:184-192.
891 Becker, J.S., Breuer, U., Hsieh, H.F., Osterholt, T., Kumtabtim, U., Wu, B., Matusch, A., Caruso,
892 J.A., and Qin, Z. 2010. Bioimaging of metals and biomolecules in mouse heart by laser
893 ablation inductively coupled plasma mass spectrometry and secondary ion mass spectrometry.
894 *Analytical Chemistry* **82**:9528-9533.
895 Beniash, E., Ivanina, A., Lieb, N.S., Kurochkin, I., and Sokolova, I.M. 2010. Elevated level of carbon
896 dioxide affects metabolism and shell formation in oysters *Crassostrea virginica*. *Marine*
897 *Ecology Progress Series* **419**:95-108.
898 Berland, S., Marie, A., Duplat, D., Milet, C., Sire, J.Y., and Bédouet, L. 2011. Coupling proteomics
899 and transcriptomics for the identification of novel and variant forms of mollusk shell proteins:
900 a study with *P. margaritifera*. *Chembiochem* **12**:950-961.
901 Bernhard, J.M., Blanks, J.K., Hintz, C.J., and Chandler, G.T. 2004. Use of the fluorescent calcite
902 marker calcein to label foraminiferal tests. *Journal of Foraminiferal Research* **34**:96-101.
903 Bradassi, F., Cumani, F., Bressan, G., and Dupont, S. 2013. Early reproductive stages in the crustose
904 coralline alga Phymatolithon lenormandii are strongly affected by mild ocean acidification.
905 *Marine Biology* **160**:2261-2269.

906 Bray, L., Pancucci-Papadopoulou, M.A., and Hall-Spencer, J.M. 2014. Sea urchin response to rising
907 pCO_2 shows ocean acidification may fundamentally alter the chemistry of marine skeletons.
908 *Mediterranean Marine Science* **15**(3):510-519. doi: http://dx.doi.org/10.12681/mms.579
909 Butt, H.-J., Cappella, B., and Kappl, M. 2005. Force measurements with the atomic force microscope:
910 Technique, interpretation and applications. *Surface Science Reports* **59**:1-152.
911 Butt, H.-J., Jaschke, M., and Ducker, W. 1995. Measuring surface forces in aqueous electrolyte
912 solution with the atomic force microscope. *Bioelectrochemistry and Bioenergetics* **38**:191-
913 201.
914 Byrne, M., Lamare, M., Winter, D., Dworjanyn, S.A., and Uthicke, S. 2013. The stunting effect of a
915 high CO_2 ocean on calcification and development in sea urchin larvae, a synthesis from the
916 tropics to the poles. *Philosophical transactions of the Royal Society of London. Series B,*
917 *Biological sciences* **368**:20120439. doi: 10.1098
918 Byrne, M., Smith, A.M., West, S., Collard, M., Dubois, P., Graba-landry, A., and Dworjanyn, S.A.
919 2014. Warming influences Mg^{2+} content, while warming and acidification influence
920 calcification and test strength of a sea urchin. *Environmental science & technology* **48**:12620-
921 12627.
922 Cai, W.-J., Ma, Y., Hopkinson, B.M., Grottoli, A.G., Warner, M.E., Ding, Q., Hu, X., Yuan, X.,
923 Schoepf, V., Xu, H., Han, C., Melman, T.F., Hoadley, K.D., Pettay, D.T., Matsui, Y.,
924 Baumann, J.H., Levas, S., Ying, Y., and Wang, Y. 2016. Microelectrode characterization of
925 coral daytime interior pH and carbonate chemistry. *Nature Communications* **7**:11144. doi:
926 10.1038/ncomms11144
927 Carricart-Ganivet, J.P., and Barnes, D.J. 2007. Densitometry from digitized images of X-radiographs:
928 Methodology for measurement of coral skeletal density. *Journal of Experimental Marine*
929 *Biology and Ecology* **344**:67-72.
930 Chan, V.B.S., Toyofuku. T., Wetzel, G., Saraf, L., Thiyagarajan, V., and Mount, A. S. 2017.
931 Characterization of calcification events using live optical and electron microscopy techniques
932 in a marine tubeworm. *Journal of Visualized Experiments*:e55164-e55164.

933 Chan, V.B.S., Li., C., Lane, A.C., Wang, Y., Lu, X., Shih, K., Zhang, T., and Thiyagarajan, V. 2012.
934 CO_2-driven ocean acidification alters and weakens integrity of the calcareous tubes produced
935 by the serpulid tubeworm, *Hydroides elegans*. *PLOS ONE* **7**:e42718
936 Chan, V.B.S., Toyofuku, T., Wetzel, G., Saraf, L., Thiyagarajan, V., and Mount, A.S. 2015a. Direct
937 deposition of crystalline aragonite in the controlled biomineralization of the calcareous
938 tubeworm. *Frontiers in Marine Science* **2**(97):1-10. doi: 10.3389/fmars.2015.00097
939 Chan, V.B.S., Vinn, O., Li, C., Lu, X., Kudryavtsev, A.B., Schopf, J.W., Shih, K., Zhang, T., and
940 Thiyagarajan, V. 2015b. Evidence of compositional and ultrastructural shifts during the
941 development of calcareous tubes in the biofouling tubeworm, *Hydroides elegans*. *Journal of*
942 *structural biology* **189**:230-237.
943 Chatzinikolaou, E., Grigoriou, P., Keklikoglou, K., Faulwetter, S., and Papageorgiou, N. 2017. The
944 combined effects of reduced pH and elevated temperature on the shell density of two
945 gastropod species measured using micro-CT imaging. *ICES Journal of Marine Science:*
946 *Journal du Conseil* **74**:1135-1149.
947 Collard, M., Rastrick, S.P.S., Calosi, P., Demolder, Y., Dille, J., Findlay, H.S., Hall-Spencer, J.M.,
948 Milazzo, M., Moulin, L., Widdicombe, S., Dehairs, F., and Dubois, P. 2016. The impact of
949 ocean acidification and warming on the skeletal mechanical properties of the sea urchin
950 *Paracentrotus lividus* from laboratory and field observations. *ICES Journal of Marine*
951 *Science* **73**:727-738.
952 Comeau, S., Cornwall, C.E., and McCulloch, M.T. 2017a. Decoupling between the response of coral
953 calcifying fluid pH and calcification to ocean acidification. *Scientific Reports* **7**:7573.
954 doi:10.1038/s41598-017-08003-z
955 Comeau, S., Tambutte, E., Carpenter, R.C., Edmunds, P.J., Evensen, N.R., Allemand, D., Ferrier-
956 Pages, C., Tambutte, S., and Venn, A.A. 2017b. Coral calcifying fluid pH is modulated by
957 seawater carbonate chemistry not solely seawater pH. *Proceedings of the Royal Society B-*
958 *Biological Sciences* **284**: 20161669. doi: 10.1098/rspb.2016.1669

959 Cooper, T.F., De'Ath, G., Fabricius, K.E., and Lough, J.M. 2008. Declining coral calcification in
960 massive Porites in two nearshore regions of the northern Great Barrier Reef. *Global Change*
961 *Biology* **14**:529-538.
962 Cummings, V., Hewitt, J., Van Rooyen, A., Currie, K., Beard, S., Thrush, S., Norkko, J., Barr, N.,
963 Heath, P., Halliday, N.J., Sedcole, R., Gomez, A., McGraw, C., and Metcalf, V. 2011. Ocean
964 acidification at high latitudes: potential effects on functioning of the Antarctic bivalve
965 *Laternula elliptica*. *PLOS ONE* **6**:e16069
966 Cyronak, T., Schulz, K.G., and Jokiel, P.L. 2016. The Omega myth: what really drives lower
967 calcification rates in an acidifying ocean. *ICES Journal of Marine Science* **73**:558-562.
968 Dalbeck, P., Cusack, M., Dobson, P.S., Allison, N., Fallick, A.E., and Tudhope, A.W. 2011.
969 Identification and composition of secondary meniscus calcite in fossil coral and the effect on
970 predicted sea surface temperature. *Chemical Geology* **280**:314-322.
971 Davies, P.S. 1989. Short-term growth measurements of corals using an accurate buoyant weighing
972 technique. *Marine Biology* **101**:389-395.
973 de Nooijer, L.J., Toyofuku, T., Oguri, K., Nomaki, H., and Kitazato, H. 2008. Intracellular pH
974 distribution in foraminifera determined by the fluorescent probe HPTS. *Limnology and*
975 *Oceanography: Methods* **6**:610-618.
976 De Wit, P., Dupont, S., and Thor, P. 2016. Selection on oxidative phosphorylation and ribosomal
977 structure as a multigenerational response to ocean acidification in the common copepod
978 Pseudocalanus acuspes. *Evolutionary Applications* **9**:1112-1123.
979 De Wit, P., Durland, E., Ventura, A., and Langdon, C.J. 2018. Gene expression correlated with delay
980 in shell formation in larval Pacific oysters (*Crassostrea gigas*) exposed to experimental ocean
981 acidification provides insights into shell formation mechanisms. *Bmc Genomics* **19**:160.
982 deVries, M.S., Webb, S.J., Tu, J., Cory, E., Morgan, V., Sah, R.L., Deheyn, D.D., and Taylor, J.R.A.
983 2016. Stress physiology and weapon integrity of intertidal mantis shrimp under future ocean
984 conditions. *Scientific Reports* **6**:38637.

985 Dickinson, G.H., Ivanina, A.V., Matoo, O.B., Portner, H.O., Lannig, G., Bock, C., Beniash, E., and
986 Sokolova, I.M. 2012a. Interactive effects of salinity and elevated CO_2 levels on juvenile
987 eastern oysters, *Crassostrea virginica*. *The Journal of Experimental Biology* **215**:29-43.
988 Dickinson, G.H., Ivanina, A.V., Matoo, O.B., Pörtner, H.O., Lannig, G., Bocl, C., Beniash, E., and
989 Sokolova, I.M. 2012b. Interactive effects of salinity and elevated CO_2 levels on juvenile
990 eastern oysters, *Crassostrea virginica*. *Journal of Experimental Biology* **215**:29-43.
991 Dineshram, R., Sharma, R., Chandramouli, K., Yalamanchili, H.K., Chu, I., and Thiyagarajan, V.
992 2015. Comparative and quantitative proteomics reveal the adaptive strategies of oyster larvae
993 to ocean acidification. *Proteomics* **15**:4120-4134.
994 Doney, S.C., Fabry, V.J., Feely, R.A., and Kleypas, J.A. 2009. Ocean acidification: the other CO_2
995 problem. *Annual Review of Marine Science* **1**:169-192.
996 Drake, J.L., Mass, T., Haramaty, L., Zelzion, E., Bhattacharya, D., and Falkowski, P.G. 2013.
997 Proteomic analysis of skeletal organic matrix from the stony coral *Stylophora pistillata*.
998 *Proceedings of the National Academy of Sciences* **110**:3788-3793.
999 Dwyer, G.S., Cronin, T.M. and Baker, P.A. 2013. Trace elements in marine ostracodes. In
1000 J.A.Holmes & A.R.Chivas (eds) *The Ostracoda: Applications in Quaternary Research.*
1001 *Geophys. Monogr. Series.*, AGU, Washington. Pages 205-225.
1002 Eichner, M.J., Klawonn, I., Wilson, S.T., Littmann, Whitehouse, S.M.J., Church, M.J., Kuypers,
1003 M.M.M., Karl, D.M., and Ploug, H. 2017. Chemical microenvironments and single-cell
1004 carbon and nitrogen uptake in field-collected colonies of Trichodesmium under different
1005 pCO_2. *The Isme Journal* **11**:1305.
1006 Eisenstein, N.M., Cox, S.C., Williams, R.L., Stapley, S.A., and Grover, L.M. 2016. Bedside,
1007 benchtop, and bioengineering: physicochemical imaging techniques in biomineralization.
1008 *Advanced healthcare materials* **5**:507-528.
1009 Elderfield, H., Bertram, C.J., and Erez, J. 1996. A biomineralization model for the incorporation of
1010 trace elements into foraminiferal calcium carbonate. *Earth and Planetary Science Letters*
1011 **142**:409-423.

1012 Erez, J. 1978. Vital effect on stable-isotope composition seen in foraminifera and coral skeletons.
1013 *Nature* **273**:199.
1014 Falini, G., Weiner, S., and Addadi, L. 2003. Chitin-silk fibroin interactions: relevance to calcium
1015 carbonate formation in invertebrates. *Calcified tissue international* **72**:548-554.
1016 Fang, J.K., Schoenberg, C.H., Kline, D.I., Hoegh-Guldberg, O., and Dove, S. 2013. Methods to
1017 quantify components of the excavating sponge *Cliona orientalis* Thiele, 1900. *Marine*
1018 *Ecology* **34**:193-206.
1019 Fantazzini, P., Mengoli, S., Pasquini, L., Bortolotti, V., Brizi, L., Mariani, M., Di Giosia, M.,
1020 Fermani, S., Capaccioni, B., Caroselli, E., Prada, F., Zaccanti, F., Levy, O., Dubinsky, Z,
1021 Kaandorp, J.A., Konglerd, P., Hammel, J.U., Dauphin, Y., Cuif, J.-P., Weaver, J.C.,
1022 Fabricius, K.E., Wagermaier, W., Fratzl, P., Falini, G., and Goffredo, S. 2015. Gains and
1023 losses of coral skeletal porosity changes with ocean acidification acclimation. *Nature*
1024 *Communications* **6**:7785. doi: 10.1038/ncomms8785
1025 Feder, M.E., and Walser, J.C. 2005. The biological limitations of transcriptomics in elucidating stress
1026 and stress responses. *Journal of evolutionary biology* **18**:901-910.
1027 Fietzke, J., Heinemann, A., Taubner, I., Böhm, F., Erez, J., and Eisenhauer, A. 2010. Boron isotope
1028 ratio determination in carbonates via LA-MC-ICP-MS using soda-lime glass standards as
1029 reference material. *Journal of Analytical Atomic Spectrometry* **25**:1953-1957.
1030 Fitzer, S. Chung, C.P., Maccherozzi, F., Dhesi, S.S., Kamenos, N.A., Phoenix, V.R., and Cusack,
1031 M.2016. Biomineral shell formation under ocean acidification: a shift from order to chaos.
1032 *Scientific Reports* **6**:21076. doi: 10.1038/srep21076
1033 Fitzer, S.C., Cusack, M., Phoenix, V.R., and Kamenos, N.A. 2014a. Ocean acidification reduces the
1034 crystallographic control in juvenile mussel shells. *Journal of structural biology* **188**:39-45.
1035 Fitzer, S.C., Phoenix, V.R., Cusack, M., and Kamenos, N.A. 2014b. Ocean acidification impacts
1036 mussel control on biomineralisation. *Scientific Reports* **4**:6218. doi: 10.1038/srep06218
1037 Fitzer, S.C., Vittert, L., Bowman, A., Kamenos, N.A., Phoenix, V.R., and Cusack, M. 2015a. Ocean
1038 acidification and temperature increase impact mussel shell shape and thickness: problematic
1039 for protection? *Ecology and Evolution* **5**:4875-4884.

1040 Fitzer, S.C., Zhu, W., Tanner, K.E., Kamenos, N.A., Phoenix, V.R., and Cusack, M. 2015b. Ocean
1041 acidification alters the material properties of *Mytilus edulis* shells. *Journal of the Royal*
1042 *Society Interface* **12**:20141227.
1043 Freeman, A.S., and Byers J.E. 2006. Divergent induced responses to an invasive predator in marine
1044 mussel populations. *Science* **313**:831-833.
1045 Frieder, C.A., Applebaum, S.L., Pan, T.C.F., Hedgecock, D, and Manahan, D.T. 2016. Metabolic cost
1046 of calcification in bivalve larvae under experimental ocean acidification. *ICES Journal of*
1047 *Marine Science*. **74**(4):941-954. doi:https://doi.org/10.1093/icesjms/fsw213
1048 Fu, J.M., He, C., Xia, B., Li, Y., Feng, Q., Yin, Q.F., Shi, X.H., Feng, X., Wang, H.T., and Yao, H.M.
1049 2016. c-axis preferential orientation of hydroxyapatite accounts for the high wear resistance
1050 of the teeth of black carp (*Mylopharyngodon piceus*). *Scientific Reports* **6:**23509. doi:
1051 10.1038/srep23509
1052 Furla, P., Galgani, I., Durand, I., and Allemand, D. 2000. Sources and mechanisms of inorganic
1053 carbon transport for coral calcification and photosynthesis. *Journal of Experimental Biology*
1054 **203**:3445-3457.
1055 Furuhashi, T., Beran, A., Blazso, M., Czegeny, Z., Schwarzinger, C., and Steiner, G. 2009. Pyrolysis
1056 GC/MS and IR spectroscopy in chitin analysis of molluscan shells. *Bioscience,*
1057 *biotechnology, and biochemistry* **73**:93-103.
1058 Gao, K., Ruan, Z., Villafañe, V.E., Gattuso, J.-P., and Helbling, E.W. 2009. Ocean acidification
1059 exacerbates the effect of UV radiation on the calcifying phytoplankter *Emiliania huxleyi*.
1060 *Limnology and Oceanography* **54**:1855-1862.
1061 Gazeau, F., Quiblier, C., Jansen, J.M., Gattuso, J.-P., Middelburg, J.J., and Heip, C.H.R. 2007. Impact
1062 of elevated CO_2 on shellfish calcification. *Geophysical Research Letters* **34**(7): L07603.
1063 Ghosh, P., Adkins, J., Affek, H., Balta, B., Guo, W., Schauble, E.A., Schrag, D., and Eiler, J.M. 2006.
1064 13C–18O bonds in carbonate minerals: A new kind of paleothermometer. *Geochimica et*
1065 *Cosmochimica Acta* **70**:1439-1456.

1066 Glas, M.S., Fabricius, K.E., de Beer, D., and Uthicke, S. 2012a. The O_2, pH and Ca^{2+}
1067 microenvironment of benthic foraminifera in a high CO_2 world. *PLOS ONE* **7**:e50010.
1068 doi:10.1371/journal.pone.0050010
1069 Glas, M.S., Langer, G., and Keul, N. 2012b. Calcification acidifies the microenvironment of a benthic
1070 foraminifer (Ammonia sp.). *Journal of Experimental Marine Biology and Ecology* **424-**
1071 **425**:53-58.
1072 Goffredo, S., Prada, F., Caroselli, E., Capaccioni, B., Zaccanti, F., Pasquini, L., Fantazzini, P.,
1073 Fermani, S., Reggi, M., Levy, O., Fabricius, K.E., Dubinsky, Z., and Falini, G. 2014.
1074 Biomineralization control related to population density under ocean acidification. *Nature*
1075 *Clim. Change* **4**:593-597.
1076 Gong, Y.U.T., Killian, C.E., Olson, I.C., Appathurai, N.P., Amasino, A.L., Martin, M.C., Holt, L.J.,
1077 Wilt, F.H., and Gilbert, P.U.P.A. 2012. Phase transitions in biogenic amorphous calcium
1078 carbonate. *PNAS* **109**:6088-6093.
1079 Guidetti, P., and Mori, M. 2005. Morpho-functional defences of Mediterranean sea urchins,
1080 *Paracentrotus lividus* and *Arbacia lixula*, against fish predators. *Marine Biology* **147**:797-
1081 802.
1082 Guo, W., Mosenfelder, J.L., Goddard III, W.A., and Eiler, J.M. 2009. Isotopic fractionations
1083 associated with phosphoric acid digestion of carbonate minerals: Insights from first-principles
1084 theoretical modeling and clumped isotope measurements. *Geochimica et Cosmochimica Acta*
1085 **73**:7203–7225.
1086 Hahn, S., Rodolfo-Metalpa, R., Griesshaber, E., Schmahl, W.W., Buhl, D., Hall-Spencer, J.M.,
1087 Baggini, C., Fehr, K.T., and Immenhauser, A. 2012. Marine bivalve shell geochemistry and
1088 ultrastructure from modern low pH environments: environmental effect versus experimental
1089 bias. *Biogeosciences* **9**:1897-1914.
1090 Harney, E., Artigaud, S., Le Souchu, P., Miner, P., Corporeau, C., Essid, H., Pichereau, V., and
1091 Nunes, F.L.D. 2016. Non-additive effects of ocean acidification in combination with warming
1092 on the larval proteome of the Pacific oyster, *Crassostrea gigas*. *Journal of proteomics*
1093 **135**:151-161.

1094 Hemming, N.G., and Hanson, G.N. 1992. Boron isotopic composition and concentration in modern
1095 marine carbonates. *Geochimica et Cosmochimica Acta* **56**:537-543.
1096 Herler, J., and Dirnwöber, M. 2011. A simple technique for measuring buoyant weight increment of
1097 entire, transplanted coral colonies in the field. *Journal of Experimental Marine Biology and*
1098 *Ecology* **407**:250-255.
1099 Hofmann, G.E., O'Donnell, M.J., and Todgham, A.E. 2008. Using functional genomics to explore the
1100 effects of ocean acidification on calcifying marine organisms. *Marine Ecology Progress*
1101 *Series* **373**:219-226.
1102 Huang, S., Chaudhary, K., and Garmire, L.X. 2017. More is better: recent progress in multi-omics
1103 data integration methods. *Frontiers in Genetics* **8**(84):1-12. doi:
1104 https://doi.org/10.3389/fgene.2017.00084
1105 Iglesias-Rodriguez, M.D., Halloran, P.R., Rickaby, R.E.M., Hall, I.R., Colmenero-Hidalgo, E.,
1106 Gittins, J.R., Green, D.R.H., Tyrrell, T., Gibbs, S.J., von Dassow, P., Rehm, E., Armbrust,
1107 E.V., and Boessenkool, K.P. 2008. Phytoplankton calcification in a high-CO_2 world. *Science*
1108 **320**:336-340.
1109 Jeffree, R.A., Markich, S.J., Lefebvre, F., Thellier, M., and Ripoll, C. 1995. Shell microlaminations of
1110 the freshwater bivalveHyridella depressa as an archival monitor of manganese water
1111 concentration: Experimental investigation by depth profiling using secondary ion mass
1112 spectrometry (SIMS). *Experientia* **51**:838-848.
1113 Jokiel, P.L., Rodgers, K.S., Kuffner, I.B., Andersson, A.J., Cox, E.F., and Mackenzie, F.T. 2008.
1114 Ocean acidification and calcifying reef organisms: a mesocosm investigation. *Coral Reefs*
1115 **27**:473-483.
1116 Joubert, C., Piquemal, D., Marie, B., Manchon, L., Pierrat, F., Zanella-Cléon, I., Cochennec-Laureau,
1117 N., Gueguen, Y., and Montagnani, C. 2010. Transcriptome and proteome analysis of Pinctada
1118 margaritifera calcifying mantle and shell: focus on biomineralization. *Bmc Genomics* **11**:613.
1119 Kamenos, N.A., Burdett, H.L., Aloisio, E., Findlay, H.S., Martin, S., Longobone, C., Dunn,
1120 J.Widdicombe, S., and Calosi, P. 2013. Coralline algal structure is more sensitive to rate,
1121 rather than the magnitude, of ocean acidification. *Global Change Biology* **19**:3621–3628.

1122 Katano, H., Takakuwa, M., Hayakawa, H., and Kimoto, H. 2016. Determination of chitin based on the
1123 colorimetric assay of glucosamine in acid hydrolysate. *Analytical Sciences.* **32**: 701-703.
1124 Keul, N., Langer, G., de Nooijer, L.J., Nehrke, G., Reichart, G.J., and Bijma, J. 2013. Incorporation of
1125 uranium in benthic foraminiferal calcite reflects seawater carbonate ion concentration.
1126 *Geochemistry, Geophysics, Geosystems* **14**:102-111.
1127 Khalifa, G.M., Kirchenbuechler, D., Koifman, N., Kleinerman, O., Talmon, Y., Elbaum, M., Addadi,
1128 L., Weiner, S., and Erez, J. 2016. Biomineralization pathways in a foraminifer revealed using
1129 a novel correlative cryo-fluorescence–SEM–EDS technique. *Journal of structural biology*
1130 **196**:155-163.
1131 Kikuchi, S. 1928. Diffraction of cathode rays by mica. *Proceedings of the Imperial Academy* **4**:354-
1132 356.
1133 Krief, S., Hendy, E.J., Fine, M., Yam, R., Meibom, A., Foster, G.L., and Shemesh, A. 2010.
1134 Physiological and isotopic responses of scleractinian corals to ocean acidification.
1135 *Geochimica et Cosmochimica Acta* **74**:4988-5001.
1136 Kruzic, J.J., Kim, D.K., Koester, K.J., and Ritchie, R.O. 2009. Indentation techniques for evaluating
1137 the fracture toughness of biomaterials and hard tissues. *Journal of the Mechanical Behavior*
1138 *of Biomedical Materials* **2**:384-395.
1139 Kunitake, M.E., Baker, S.P., and Estroff, L.A. 2012. The effect of magnesium substitution on the
1140 hardness of synthetic and biogenic calcite. *MRS Communications* **2**:113-116.
1141 Kunitake, M.E., Mangano, L.M., Peloquin, J.M., Baker, S.P., and Estroff, L.A. 2013. Evaluation of
1142 strengthening mechanisms in calcite single crystals from mollusk shells. *Acta Biomaterialia*
1143 **9**:5353-5359.
1144 Langdon, C., and Atkinson, M.J. 2005. Effect of elevated pCO_2 on photosynthesis and calcification of
1145 corals and interactions with seasonal change in temperature/irradiance and nutrient
1146 enrichment. *Journal of Geophysical Research: Oceans* **110**:C09S07.
1147 Langdon, C., Takahashi, T., Sweeney, C., Chipman, D., Goddard, J., Marubini, F., Aceves, H.,
1148 Barnett, H., and Atkinson, M.J. 2000. Effect of calcium carbonate saturation state on the
1149 calcification rate of an experimental coral reef. *Global Biogeochemical Cycles* **14**:639-654.

1150 Langer, G., Nehrke, G., Baggini, C., Rodolfo-Metalpa, R., Hall-Spencer, J.M., and Bijma, J. 2014.
1151 Limpets counteract ocean acidification induced shell corrosion by thickening of aragonitic
1152 shell layers. *Biogeosciences* **11**:7363-7368.
1153 Lawn, B.R., Evans, A., and Marshall, D. 1980. Elastic/plastic indentation damage in ceramics: the
1154 median/radial crack system. *Journal of the American Ceramic Society* **63**:574-581.
1155 Lear, C.H., Elderfield, H., and Wilson, P.A. 2000. Cenozoic deep-sea temperatures and global ice
1156 volumes from Mg/Ca in benthic foraminiferal calcite. *Science* **287**:269-272.
1157 Lee, C.G., Da Silva, C.A., Dela Cruz, C.S., Ahangari, F., Ma, B., Kang, M.J., He, C.H., Takyar, S.,
1158 and Elias, J.A. 2011. Role of chitin and chitinase/chitinase-like proteins in inflammation,
1159 tissue remodeling, and injury. *Annual Review of Physiology* **73**:479-501.
1160 Leung, J.Y., Russell, B.D., and Connell, S.D. 2017. Mineralogical plasticity acts as a compensatory
1161 mechanism to the impacts of ocean acidification. *Environmental science & technology*
1162 **51**(5):2652-2659.
1163 Levi-Kalisman, Y., Falini, G., Addadi, L., and Weiner, S. 2001. Structure of the nacreous organic
1164 matrix of a bivalve mollusk shell examined in the hydrated state using cryo-TEM. *Journal of*
1165 *structural biology* **135**:8-17.
1166 Lewis, B., and Diaz-Pulido, G. 2017. Suitability of three fluorochrome markers for obtaining in situ
1167 growth rates of coralline algae. *Journal of Experimental Marine Biology and Ecology* **490**:64-
1168 73.
1169 Li, C., Chan, V.B.S., He, C., Meng, Y., Yao, H., Shih, K., and Thiyagarajan, V. 2014. Weakening
1170 mechanisms of the serpulid tube in a high-CO_2 world. *Environmental science & technology*
1171 **48**:14158-14167.
1172 Li, C., Meng, Y., He, C., Chan, V.B.S., Yao, H., and Thiyagarajan, V. 2016. Mechanical robustness
1173 of the calcareous tubeworm *Hydroides elegans*: warming mitigates the adverse effects of
1174 ocean acidification. *Biofouling* **32**:191-204.
1175 Li, Y., Zhuang, S., Wu, Y., Ren, H., Cheng, F., Lin, X., Wang, K., Beardall, J., and Gao, K. 2015.
1176 Ocean acidification modulates expression of genes and physiological performance of a marine
1177 diatom. *Biogeosciences Discuss.* **2015**:15809-15833.

1178 Limbeck, A., Bonta, M., and Nischkauer, W. 2017. Improvements in the direct analysis of advanced
1179 materials using ICP-based measurement techniques. *Journal of Analytical Atomic*
1180 *Spectrometry* **32**:212-232.
1181 Lombardi, C., Cocito, S., Gambi, M.C., and Taylor, P.D. 2015. Morphological plasticity in
1182 a calcifying modular organism: evidence from an *in situ* transplant experiment in a natural
1183 CO_2 vent system. *Royal Society Open Science* **2**(2):140413. doi: 10.1098/rsos.140413.
1184 Luo, Y.-J., Takeuchi, T., Koyanagi, R., Yamada, L., Kanda, M., Khalturina, M., Fujie, M., Yamasaki,
1185 S.-I., Endo, K., and Satoh, N. 2015. The *Lingula* genome provides insights into brachiopod
1186 evolution and the origin of phosphate biomineralization. *Nature Communications* **6**: 8301.
1187 doi: 10.1038/ncomms9301
1188 Mackenzie, C.L., Ormondroyd, G.A., Curling, S.F., Ball, R.J., Whiteley, N.M., and Malham, S.K.
1189 2014. Ocean warming, more than acidification, reduces shell strength in a commercial
1190 shellfish species during food limitation. *PLOS ONE* **9**:e86764.
1191 doi:10.1371/journal.pone.0086764
1192 Mann, M., and Jensen, O.N. 2003. Proteomic analysis of post-translational modifications. *Nature*
1193 *biotechnology* **21**:255-261.
1194 Marie, B., Le Roy, N., Zanella-Cléon, I., Becchi, M., and Marin, F. 2011. Molecular evolution of
1195 mollusc shell proteins: insights from proteomic analysis of the edible mussel *Mytilus*. *Journal*
1196 *of molecular evolution* **72**:531-546.
1197 Marie, B., Marie, A., Jackson, D.J., Dubost, L., Degnan, B.M., Milet, C., and Marin, F. 2010.
1198 Proteomic analysis of the organic matrix of the abalone *Haliotis asinina* calcified shell.
1199 *Proteome Science* **8**:54. doi: 10.1186/1477-5956-8-54
1200 Marsh, J.A. 1970. Primary Productivity of Reef-Building Calcareous Red Algae. *Ecology* **51**:255-263.
1201 Martin, P., Goodkin, N.F., Stewart, J.A., Foster, G.L., Sikes, E.L., White, H.K., Hennige, S., and
1202 Roberts, J.M. 2016. Deep-sea coral δ13C: A tool to reconstruct the difference between
1203 seawater pH and δ11B-derived calcifying fluid pH. *Geophysical Research Letters* **43**:299-
1204 308.

1205 Martin, P.A., and Lea, D.W. 2002. A simple evaluation of cleaning procedures on fossil benthic
1206 foraminiferal Mg/Ca. *Geochemistry, Geophysics, Geosystems* **3**:1-8.
1207 Marxen, J.C., Nimtz, M., Becker, W., and Mann, K. 2003. The major soluble 19.6 kDa protein of the
1208 organic shell matrix of the freshwater snail *Biomphalaria glabrata* is an N-glycosylated
1209 dermatopontin. *Biochimica et Biophysica Acta (BBA)-Proteins and Proteomics* **1650**:92-98.
1210 McConnaughey, T.A., and Gillikin, D.P. 2008. Carbon isotopes in mollusk shell carbonates. *Geo-*
1211 *Marine Letters* **28**:287-299.
1212 McEnery, M., and Lee, J.J. 1970. Tracer studies on calcium and strontium mineralization and mineral
1213 cycling in two species of foraminifera, *Rosalina leei* and *Spiroloculina hyalina*. *Limnology*
1214 *and Oceanography* **15**:173-182.
1215 Melbourne, L.A., Griffin, J., Schmidt, D.N., and Rayfield, E.J.. 2015. Potential and limitations of
1216 finite element modelling in assessing structural integrity of coralline algae under future global
1217 change. *Biogeosciences.* **12**(15): 5891-5883. doi: 10.5194/bg-12-5871-2015
1218 Melzner, F., Stange, P., Trubenbach, K., Thomsen, J., Casties, I., Panknin, U., Gorb, S.N., and
1219 Gutowska, M.A. 2011. Food supply and seawater pCO_2 impact calcification and internal shell
1220 dissolution in the blue mussel *Mytilus edulis*. *PLOS ONE* **6**:e24223. doi:
1221 10.1371/journal.pone.0024223
1222 Milano, S., Schöne, B.R., Wang, S., and Müller, W.E. 2016. Impact of high pCO_2 on shell structure of
1223 the bivalve *Cerastoderma edule*. *Marine Environmental Research* **119**:144-155.
1224 Milazzo, M., Rodolfo-Metalpa, R., Chan, V.B.S., Fine, M., Alessi, C., Thiyagarajan, V., Hall-
1225 Spencer, J.M., and Chemello, R. 2014. Ocean acidification impairs vermetid reef recruitment.
1226 *Scientific Reports* **4**:4189.
1227 Miyamoto, H., Miyashita, T., Okushima, M., Nakano, S., Morita, T., and Matsushiro, A. 1996. A
1228 carbonic anhydrase from the nacreous layer in oyster pearls. *Proceedings of the National*
1229 *Academy of Sciences* **93**:9657-9660.
1230 Molina, R., Hanlon, S., Savidge, T., Bogan, A., and Levine, J. 2005. Buoyant weight technique:
1231 application to freshwater bivalves. *American Malacological Bulletin* **20**:49-53.

1232 Müller, M.N., Kısakürek, B., Buhl, D., Gutperlet, R., Kolevica, A., Riebesell, U., Stoll, H., and
1233 Eisenhauer, A. 2011. Response of the coccolithophores *Emiliania huxleyi* and *Coccolithus*
1234 *braarudii* to changing seawater Mg^{2+} and Ca^{2+} concentrations: Mg/Ca, Sr/Ca ratios and
1235 δ44/40Ca, δ26/24Mg of coccolith calcite. *Geochimica et Cosmochimica Acta* **75**:2088-2102.
1236 Naddafi, R., and Rudstam, L.G. 2014. Predator induced morphological change in dreissenid mussels:
1237 implications for species replacement. *Freshwater Biology* **59**:703-713.
1238 Nakayama, S., Suzuki, M., Endo, H., Limura, K., Kinoshita, S., Watabe, S., Kogure, T., and
1239 Nagasawa, H. 2013. Identification and characterization of a matrix protein (PPP-10) in the
1240 periostracum of the pearl oyster, *Pinctada fucata*. *FEBS open bio* **3**:421-427.
1241 Nellist, P.D., Chisholm, M.F., Dellby, N., Krivanek, O.L., Murfitt, M.F., Szilagyi, Z.S., Lupini, A.R.,
1242 Borisevich, A., Sides, W.H., and Pennycook, S.J. 2004. Direct sub-angstrom imaging of a
1243 crystal lattice. *Science* **305**:1741-1741.
1244 Newbury, D.E. 1998. Trace element detection at nanometer scale spatial resolution. *Microscopy*
1245 **47**:407-418.
1246 Nimer, N.A., and Merrett, M.J. 1993. Calcification rate in *Emiliania huxleyi* Lohmann in response to
1247 light, nitrate and availability of inorganic carbon. *New Phytologist* **123**:673-677.
1248 Nishikawa, S., and Kikuchi, S. 1928. Diffraction of cathode rays by calcite. *Nature* **122**:726-726.
1249 Norzagaray-López, O.C., Calderon-Aguilera, L.E., Castro-Ceseña, A.B., Hirata, G., and Hernández-
1250 Ayón, J.M. 2017. Skeletal dissolution kinetics and mechanical tests in response to
1251 morphology among coral genera. *Facies* **63**:7. doi: 10.1007/s10347-016-0488-2
1252 Not, C., Thibodeau, B., and Yokoyama, Y. 2018. Incorporation of Mg, Sr, Ba, U, and B in high-Mg
1253 calcite benthic foraminifers cultured under controlled pCO_2. *Geochemistry, Geophysics,*
1254 *Geosystems* **19**:83-98.
1255 Nudelman, F, Chen, H.H., Goldberg, H.A., Weiner, S., Addadi, L. 2007. Spiers Memorial Lecture.
1256 Lessons from biomineralization: comparing the growth strategies of mollusc shell prismatic
1257 and nacreous layers in *Atrina rigida*. *Faraday Discuss* **136**:9-25.

1258 Nürnberg, D., Bijma, J., and Hemleben, C. 1996. Assessing the reliability of magnesium in
1259 foraminiferal calcite as a proxy for water mass temperatures. *Geochimica et Cosmochimica*
1260 *Acta* **60**:803-814.
1261 Oliver, W.C., and Pharr, G.M. 1992. An improved technique for determining hardness and elastic
1262 modulus using load and displacement sensing indentation experiments. *Journal of Materials*
1263 *Research* **7**:1564-1583.
1264 Orr, J.C., Fabry, V.J., Aumont, O., Bopp, L., Doney, S.C., Feely, R.A., Gnanadesikan, A., Gruber, N.,
1265 Ishida, A., and Joos, F. 2005. Anthropogenic ocean acidification over the twenty-first century
1266 and its impact on calcifying organisms. *Nature* **437**:681-686.
1267 Paasche, E. 1963. The adaptation of the carbon-14 method for the measurement of coccolith
1268 production in *Coccolithus huxleyi*. *Physiologia Plantarum* **16**:186-200.
1269 Pan, T.C.F., Applebaum, S.L., and Manahan, D.T. 2015. Experimental ocean acidification alters the
1270 allocation of metabolic energy. *Proceedings of the National Academy of Sciences* **112**:4696-
1271 4701.
1272 Parkinson, D., Curry, G.B., Cusack, M., and Fallick, A.E. 2005. Shell structure, patterns and trends of
1273 oxygen and carbon stable isotopes in modern brachiopod shells. *Chemical Geology* **219**:193-
1274 235.
1275 Pearson, F., Marchessault, R., and Liang, C. 1960. Infrared spectra of crystalline polysaccharides. V.
1276 Chitin. *Journal of Polymer Science* **43**:101-116.
1277 Perez-Huerta, A., and Cusack, M. 2009. Optimizing electron backscatter diffraction of carbonate
1278 biominerals-resin type and carbon coating. *Microscopy and Microanalysis* **15**:197-203.
1279 Pérez-Huerta, A., Cusack, M., Jeffries, T.E., and Williams, C.T. 2008. High resolution distribution of
1280 magnesium and strontium and the evaluation of Mg/Ca thermometry in Recent brachiopod
1281 shells. *Chemical Geology* **247**:229-241.
1282 Politi, Y., Levi-Kalisman, Y., Raz, S., Wilt, F., Addadi, L., Weiner, S., and Sagi, I. 2006. Structural
1283 characterization of the transient amorphous calcium carbonate precursor phase in sea urchin
1284 embryos. *Advanced Functional Materials* **16**:1289-1298.

1285 Politi, Y., Metzler, R.A., Abrecht, M., Gilbert, B., Wilt, F.H., Sagi, I., Addadi, L., Weiner, S., and
1286 Gilbert, P.U.P.A. 2008. Transformation mechanism of amorphous calcium carbonate into
1287 calcite in the sea urchin larval spicule. *Proceedings of the National Academy of Sciences of*
1288 *the United States of America* **105**:17362-17366.
1289 Rae, J.W.B., Foster, G.L., Schmidt, D.N., and Elliott, T. 2011. Boron isotopes and B/Ca in benthic
1290 foraminifera: Proxies for the deep ocean carbonate system. *Earth and Planetary Science*
1291 *Letters* **302**:403-413.
1292 Ragazzola, F., Foster, L.C., Form, A., Anderson, P.S.L., Hansteen, T.H., and Fietzke, J. 2012. *Global*
1293 *Change Biology.* **18**(9): 2804-2812. doi: 10.1111/j.1365-2486.2012.02756.x
1294 Reynaud, S., Leclercq, N., Romaine-Lioud, S., Ferrier-Pages, C., Jaubert, J., and Gattuso, J. P. 2003.
1295 Interacting effects of CO_2 partial pressure and temperature on photosynthesis and calcification
1296 in a scleractinian coral. *Global Change Biology* **9**:1660-1668.
1297 Riebesell, U., Zondervan, I., Rost, B., Tortell, P.D., Zeebe, R.E., and Morel, F.M.M. 2000. Reduced
1298 calcification of marine plankton in response to increased atmospheric CO_2. *Nature* **407**:364-
1299 367.
1300 Ries, J.B., Cohen, A.L., and McCorkle, D.C. 2009. Marine calcifiers exhibit mixed responses to CO_2-
1301 induced ocean acidification. *Geology* **37**:1131-1134.
1302 Rodolfo-Metalpa, R., Houlbreque, F., Tambutte, E., Boisson, F., Baggini, C., Patti, F.P., Jeffree, R.,
1303 Fine, M., Foggo, A., Gattuso, J.P., and Hall-Spencer, J.M. 2011. Coral and mollusc resistance
1304 to ocean acidification adversely affected by warming. *Nature Clim. Change* **1**:308-312.
1305 Rodolfo-Metalpa, R., Montagna, P., Aliani, S., Borghini, M., Canese, S., Hall-Spencer, J.M., Foggo,
1306 A., Milazzo, M., Taviani, M., and Houlbrèque, F. 2015. Calcification is not the Achilles' heel
1307 of cold-water corals in an acidifying ocean. *Global Change Biology* **21**:2238-2248.
1308 Roleda, M.Y., Boyd, P.W., and Hurd, C.L. 2012. Before ocean acidification: calcifier chemistry
1309 lessons. *Journal of Phycology* **48**:840-843.
1310 Rühl, S., Calosi, P., Faulwetter, S., Keklikoglou, K., Widdicombe, S., and Queirós, A.M. 2017. Long-
1311 term exposure to elevated pCO_2 more than warming modifies early-life shell growth in a
1312 temperate gastropod. *ICES Journal of Marine Science* **74**:1113-1124.

1313 Sabatier, P., Reyss, J.L., Hall-Spencer, J.M., Colin, C., Frank, N., Tisnérat-Laborde, N., Bordier, L.,
1314 and Douville, E. 2012. ^{210}Pb-^{226}Ra chronology reveals rapid growth rate of *Madrepora*
1315 *oculata* and *Lophelia pertusa* on world's largest cold-water coral reef. *Biogeosciences* **9**:1253-
1316 1265.
1317 Samata, T., Hayashi, N., Kono, M., Hasegawa, K., Horita, C., and Akera, S. 1999. A new matrix
1318 protein family related to the nacreous layer formation of *Pinctada fucata*. *FEBS letters*
1319 **462**:225-229.
1320 Satoh, M., Iwamoto, K., Suzuki, I., and Shiraiwa, Y. 2009. Cold stress stimulates intracellular
1321 calcification by the coccolithophore, *Emiliania huxleyi* (Haptophyceae) under phosphate-
1322 deficient conditions. *Marine biotechnology* **11**:327-333.
1323 Schoepf, V., Hu, X., Holcomb, M., Cai, W.J., Li, Q., Wang, Y., Xu, H., Warner, M.E., Melman, T.F.,
1324 Hoadley, K.D., Pettay, D.T., Matsui, Y., Baumann, J.H., and Grottoli, A.G. 2017. Coral
1325 calcification under environmental change: a direct comparison of the alkalinity anomaly and
1326 buoyant weight techniques. *Coral Reefs* **36**:13-25.
1327 Sikes, C.S., Wheeler, A.P., Wierzbicki, A., Mount, A.S., and Dillaman, R.M. 2000. Nucleation and
1328 growth of calcite on native versus pyrolyzed oyster shell folia. *Biological Bulletin* **198**:50-66.
1329 Sinclair, D.J. 2005. Correlated trace element “vital effects” in tropical corals: A new geochemical tool
1330 for probing biomineralization. *Geochimica et Cosmochimica Acta* **69**:3265-3284.
1331 Singh, S.K., and Sigworth, F.J. 2015. Cryo-EM: Spinning the Micelles Away. *Structure* **23**:1561. doi:
1332 10.1016/j.str.2015.08.001
1333 Spero, H.J., Bijma, J., Lea, D.W., and Bemis, B.E. 1997. Effect of seawater carbonate concentration
1334 on foraminiferal carbon and oxygen isotopes. *Nature* **390**:497-500.
1335 Stewart, J.A., Anagnostou, E., and Foster, G.L. 2016. An improved boron isotope pH proxy
1336 calibration for the deep-sea coral *Desmophyllum dianthus* through sub-sampling of fibrous
1337 aragonite. *Chemical Geology* **447**:148-160.
1338 Stumpp, M., Hu, M.Y., Melzner, F., Gutowska, M.A., Dorey, N., Himmerkus, N., Holtmann, W.C.,
1339 Dupont, S.T., Thorndyke, M.C., and Bleich, M. 2012. Acidified seawater impacts sea urchin

larvae pH regulatory systems relevant for calcification. *Proceedings of the National Academy of Sciences* **109**:18192-18197.

Suzuki, M., Iwashima, A., Tsutsui, N., Ohira, T., Kogure, T., and Nagasawa, H. 2011. Identification and characterisation of a calcium carbonate-binding protein, blue mussel shell protein (BMSP), from the nacreous layer. *Chembiochem* **12**:2478-2487.

Suzuki, M., Murayama, E., Inoue, H., Ozaki, N., Tohse, H., Kogure, T., and Nagasawa, H. 2004. Characterization of Prismalin-14, a novel matrix protein from the prismatic layer of the Japanese pearl oyster (*Pinctada fucata*). *Biochemical Journal* **382**:205-213.

Suzuki, M., and Nagasawa, H. 2013. Mollusk shell structures and their formation mechanism. *Canadian Journal of Zoology* **91**:349-366.

Suzuki, M., Sakuda, S., and Nagasawa, H. 2007. Identification of chitin in the prismatic layer of the shell and a chitin synthase gene from the Japanese pearl oyster, *Pinctada fucata*. *Bioscience, biotechnology, and biochemistry* **71**:1735-1744.

Suzuki, M., Saruwatari, K., Kogure, T., Yamamoto, Y., Nishimura, T., Kato, T., and Nagasawa, H. 2009. An acidic matrix protein, Pif, is a key macromolecule for nacre formation. *Science* **325**:1388-1390.

Takeuchi, T., Kawashima, T., Koyanagi, R., Gyoja, F., Tanaka, M., Ikuta, T., Shoguchi, E., Fujiwara, M., Shinzato, C., and Hisata, K. 2012. Draft genome of the pearl oyster *Pinctada fucata*: a platform for understanding bivalve biology. *DNA research*: **19**(2):117-30. doi: 10.1093/dnares/dss005

Tambutté, E., Tambutté, S., Segonds, N., Zoccola, D., Venn, A., Erez, J., and Allemand, D. 2012. Calcein labelling and electrophysiology: insights on coral tissue permeability and calcification. *Proceedings of the Royal Society B: Biological Sciences* **279**:19-27.

Tambutté, E., Venn, A.A., Holcomb, M., Segonds, N., Techer, N., Zoccola, D., Allemand, D., and Tambutté, S. 2015. Morphological plasticity of the coral skeleton under CO_2-driven seawater acidification. *Nature Communications* **6**:7368. doi: 10.1038/ncomms8368

1366 Taylor, J.R.A., Gilleard, J.M., Allen, M.C., and Deheyn, D.D. 2015. Effects of CO_2-induced pH
1367 reduction on the exoskeleton structure and biophotonic properties of the shrimp Lysmata
1368 californica. *Scientific Reports* **5**:10608. doi: 10.1038/srep10608
1369 Taylor, P.D., Tan A.S.H., Kudryavstev, A.B., and Schopf, J.W. 2016. Carbonate mineralogy of a
1370 tropical bryozoan biota and its vulnerability to ocean acidification. *Marine Biology Research*
1371 **12**:776-780.
1372 ter Kuile, B., Erez, J., and Padan, E. 1989. Mechanisms for the uptake of inorganic carbon by two
1373 species of symbiont-bearing foraminifera. *Marine Biology* **103**:241-251.
1374 Thompson, R.F., Walker, M., Siebert, C.A., Muench, S.P., and Ranson, N.A. 2016. An introduction to
1375 sample preparation and imaging by cryo-electron microscopy for structural biology. *Methods*
1376 **100**:3-15.
1377 Thor, P., and Dupont, S. 2015. Transgenerational effects alleviate severe fecundity loss during ocean
1378 acidification in a ubiquitous planktonic copepod. *Global Change Biology* **21**:2261-2271.
1379 Titze, B., and Genoud, C. 2016. Volume scanning electron microscopy for imaging biological
1380 ultrastructure. *Biology of the Cell* **108**:307-323.
1381 Todgham, A.E., and Hofmann, G.E. 2009. Transcriptomic response of sea urchin larvae
1382 Strongylocentrotus purpuratus to CO_2-driven seawater acidification. *Journal of Experimental*
1383 *Biology* **212**:2579-2594.
1384 Toyofuku, T., Matsuo, M.Y., De Nooijer, L.J., Nagai, Y., Kawada, S., Fujita, K., Reichart, G.J.,
1385 Nomaki, H., Tsuchiya, M., and Sakaguchi, H. 2017. Proton pumping accompanies
1386 calcification in foraminifera. *Nature Communications* **8**:14145. doi: 10.1038/ncomms14145
1387 Venn, A., Tambutté, E., Holcomb, M., Allemand, D., and Tambutté, S. 2011. Live tissue imaging
1388 shows reef corals elevate pH under their calcifying tissue relative to seawater. *PLOS ONE*
1389 **6**:e20013. doi: 10.1371/journal.pone.0020013
1390 Venn, A.A., Tambutté, E., Holcomb, M., Laurent, J., Allemand, D., and Tambutté, S. 2013. Impact of
1391 seawater acidification on pH at the tissue–skeleton interface and calcification in reef corals.
1392 *Proceedings of the National Academy of Sciences* **110**:1634-1639.

1393 Vézina, A.F., and Hoegh-Guldberg, O. 2008. Introduction: Effects of ocean acidification on marine
1394 ecosystems. *Marine Ecology Progress Series* **373**:199-201.
1395 Von Euw, S., Zhang, Q., Manichev, V., Murali, N., Gross, J., Feldman, L.C., Gustafsson, T., Flach,
1396 C., Mendelsohn, R., and Falkowski, P.G. 2017. Biological control of aragonite formation in
1397 stony corals. *Science* **356**:933-938.
1398 Wall, M., Fietzke, J., Schmidt, G.M., Fink, A., Hofmann, L.C., de Beer, D., and Fabricius, K.E. 2016.
1399 Internal pH regulation facilitates in situ long-term acclimation of massive corals to end-of-
1400 century carbon dioxide conditions. *Scientific Reports* **6**:30688. doi: 10.1038/srep30688
1401 Wang, X., Wang, M., Xu, J., Jia, Z., Liu, Z., Wang, L., and Song, L. 2017. Soluble adenylyl cyclase
1402 mediates mitochondrial pathway of apoptosis and ATP metabolism in oyster *Crassostrea*
1403 *gigas* exposed to elevated CO_2. *Fish & Shellfish Immunology* **66**:140-147.
1404 Watabe, N. 1965. Studies on shell formation: XI. Crystal—matrix relationships in the inner layers of
1405 mollusk shells. *Journal of ultrastructure research* **12**:351-370.
1406 Wehrmeister, U., Jacob, D.E., Soldati, A.L., Loges, N., Häger, T., and Hofmeister, W. 2011.
1407 Amorphous, nanocrystalline and crystalline calcium carbonates in biological materials.
1408 *Journal of Raman Spectroscopy* **42**:926-935.
1409 Wei, L., Wang, Q., Wu, H., Ji, C., and Zhao, J. 2015. Proteomic and metabolomic responses of
1410 Pacific oyster Crassostrea gigas to elevated pCO_2 exposure. *Journal of proteomics* **112**:83-94.
1411 Weiner, S., and Dove, P.M. 2003. An Overview of Biomineralization Processes and the Problem of
1412 the Vital Effect. *Reviews in Mineralogy and Geochemistry* **54**:1-29.
1413 Weiner, S., and Traub, W. 1980. X-ray diffraction study of the insoluble organic matrix of mollusk
1414 shells. *FEBS letters* **111**:311-316.
1415 Weiss, I.M., and Schönitzer, V. 2006. The distribution of chitin in larval shells of the bivalve mollusk
1416 *Mytilus galloprovincialis*. *Journal of structural biology* **153**:264-277.
1417 Wiese, S., Reidegeld, K.A., Meyer, H.E., and Warscheid, B. 2007. Protein labeling by iTRAQ: A
1418 new tool for quantitative mass spectrometry in proteome research. *Proteomics* **7**:340-350.
1419 Wilbur, K.M. 1964. Shell formation and regeneration. *In* K.M. Wilbur and C.M. Younge, (eds).
1420 *Physiology and the mollusca*. Academic Press, New York. Pages 243-282.

1421 Wilkinson, B.H. 1979. Biomineralization, paleoceanography, and the evolution of calcareous marine
1422 organisms. *Geology* **7**:524-527.
1423 Williams, P. 1985. Secondary ion mass spectrometry. *Annual Review of Materials Science* **15**:517-
1424 548.
1425 Wittmann, A.C., and Pörtner, H.O. 2013. Sensitivities of extant animal taxa to ocean acidification.
1426 *Nature Climate Change* **3**:995-1001.
1427 Wolfe, K., Smith, A.M., Trimby, P., and Byrne, M. 2013. Microstructure of the paper nautilus
1428 (Argonauta nodosa) shell and the novel application of electron backscatter diffraction (EBSD)
1429 to address effects of ocean acidification. *Marine Biology* **160**:2271-2278.
1430 Wood, H.L., Spicer, J.I., and Widdicombe, S. 2008. Ocean acidification may increase calcification
1431 rates, but at a cost. *Proceedings of the Royal Society B: Biological Sciences* **275**:1767-1773.
1432 Yokoo, N., Suzuki, M., Saruwatari, K., Aoki, H., Watanabe, K., Nagasawa, H., and Kogure, T. 2011.
1433 Microstructures of the larval shell of a pearl oyster, *Pinctada fucata*, investigated by FIB-
1434 TEM technique. *American Mineralogist* **96**:1020-1027.
1435 Zhang, C., and Zhang, R. 2006. Matrix proteins in the outer shells of molluscs. *Marine biotechnology*
1436 **8**:572-586.
1437 Zhang, G., Fang, X., Guo, X., Li, L., Luo, R., Xu, F., Yang, P., Zhang, L., Wang, X., Qi, H., Xiong,
1438 Z., Que, H., Xie, Y., Holland, P.W., Paps, J., Zhu, Y., Wu, F., Chen, Y., Wang, J., Peng, C.,
1439 Meng, J., Yang, L., Liu, J., Wen, B., Zhang, N., Huang, Z., Zhu, Q., Feng, Y., Mount, A.,
1440 Hedgecock, D., Xu, Z., Liu, Y., Domazet-Lošo, T., Du, Y., Sun, X., Zhang, S., Liu, B.,
1441 Cheng, P., Jiang, X., Li, J., Fan, D., Wang, W., Fu, W., Wang, T., Wang, B., Zhang, J., Peng,
1442 Z., Li, Y., Li, N., Wang, J., Chen, M., He, Y., Tan, F., Song, X., Zheng, Q., Huang, R., Yang,
1443 H., Du, X., Chen, L., Yang, M., Gaffney, P.M., Wang, S., Luo, L., She, Z., Ming, Y., Huang,
1444 W., Zhang, S., Huang, B., Zhang, Y., Qu, T., Ni, P., Miao, G., Wang, J., Wang, Q., Steinberg,
1445 C.E., Wang, H., Li, N., Qian, L., Zhang, G., Li, Y., Yang, H., Liu, X., Wang, J., Yin, Y.,
1446 Wang, J. 2012. The oyster genome reveals stress adaptation and complexity of shell
1447 formation. *Nature* **490**:49-54.

Zhang, S., Henehan, M.J., Hull, P.M., Reid, R.P., Hardisty, D.S., Hood, A.V.S., and Planavsky, N.J. 2017. Investigating controls on boron isotope ratios in shallow marine carbonates. *Earth and Planetary Science Letters* **458**:380-393.

Zhao, P., and Cai, W.J. 1999. pH polymeric membrane microelectrodes based on neutral carriers and their application in aquatic environments. *Anal. Chim Acta* **395**:285-291.

Table 1. Summary of established techniques on Growth and Development to measure calcification and morphology under OA conditions with details of measurements, advantages and disadvantages of each application.

Table 2. Summary of emerging techniques on Mechanical tests to investigate mechanical properties under OA conditions with details of measurements, advantages and disadvantages of each application.

Table 3. Summary of emerging techniques on Mineral composition to investigate mechanical properties under OA conditions with details of measurements, advantages and disadvantages of each application.

Table 4. Summary of emerging techniques on Cellular biomineralization mechanisms to investigate mechanical properties under OA conditions with details of measurements, advantages and disadvantages of each application.

1. Growth and development			
Technique	***Measurement(s)***	***Advantages***	***Disadvantages***
Dyes - alizarin red and calcein	• *Alizarin red stains calcium rich structures a red/light purple colour* • *Calcein stains calcium rich structures a fluorescent green colour*	• *Low cost, non-invasive* • *Track shell growth of living organisms during exposure to experiment* • *Data comparable to published work* • *Dye location can be analysed with advanced characterisation methods*	• *Alizarin red also binds free Ca* • *Calcein also binds Ca^{2+}, Mg^{2+}, Zn^{2+}* • *Is not compatible with other fluorescence techniques such as internal pH measurement* • *No mineral phase information*
SEM	• *High resolution characterisation* • *Ultrastructures of minerals*	• *Low cost* • *Data are comparable* • *Provide structural information*	• *No mineral phase information*
Buoyant weight	• *Mineral content determined from submerged weight of organism*	• *Low cost* • *Non-invasive* • *More accurate than length or area measurements* • *Mineral density changes are reflected in measurement*	• *Seawater density varies when temperature and salinity change* • *Purpose-made setup needed*
Radioactive isotopes	• *^{45}Ca incorporation rate* • *^{14}C incorporation* • *Represents mineralisation process during an experiment*	• *More accurate than length or area measurements* • *Synthetic isotopes are specific to the study*	• *Invasive acid digestion of mineral samples are needed for scintillation measurement* • *Requires handling of radioactive substances*
Total alkalinity anomaly technique	• *Alkalinity reduction surrounding an organism*	• *Low cost* • *Accurate*	• *Incubation in individual organism required*

			• *Not suitable for long-term studies*
2. Mechanical tests - Protective function or ability to survive protection			
Technique	***Measurement(s)***	***Advantages***	***Disadvantages***
Three-point bending tests	• *Elastic modulus* • *Fracture toughness*	• *Mimic predatory attack* • *Simple operation* • *Low cost*	• *Requires a tailor-made device* • *Test samples are cut into a standard size for testing*
Computed tomography	• *Shell thickness* • *Shell volume* • *Shell density*	• *3D visualisation of shell shape for morphometric analysis*	• *Hard to detect planktonic and larval samples (15 - 1000 µm per pixel)* • *Standard density calibrated with bone mineral density (BMD, in $g.cm^{-3}$)*
Finite element analysis	• *Visualize structural weakness of a material* • *Provide a numerical model for material properties*	• *Links nanoindentation data to whole sample measurements* • *Takes shell shape changes into account* • *Data can be verified by mechanical tests*	• *Requires computational skills* • *Shape information requires simpliflied experimental data* • *FEA Models need experimental verification*
Microindentation	• *Compressive force using 4- Vickers tip* • *Hardness* • *Elasticity Modulus*	• *Broader Vickers tip is less localised than nanoindentation* • *Lower cost than nanoindentation* • *Provides microscale spatial resolution*	• *Localised measurement* • *Does not represent shape and mechanical behaviour of the whole structure* • *Destructive to the sampling area of the specimen*
Nanoindentation	• *Compressive force using Berkovich tip* • *Hardness* • *Elasticity Modulus*	• *Sharper Berkovich tip enables higher spatial refinement of measurements* • *Provides both hardness and elasticity data in one measurement*	• *Localised measurement* • *Does not represent shape and mechanical behaviour of the whole structure* • *Destructive to the sampling area of the specimen*

1470

1471

1472

3. Biomineralisation mechanisms to enable growth			
Elemental analysis			
Technique	***Measurement(s)***	***Advantages***	***Disadvantages***
Inductively coupled plasma (ICP) spectrometry	• *Element to calcium ratios, e.g. Mg/Ca, Sr/Ca* • *Analyse acid digested samples*	• *Quantitative* • *Data are comparable* • *Coupling with OES, MS or AES provides different sensitivity at various costs*	• *Destructive sample preparation* • *Requires elemental standards* • *More sensitive instruments are more costly*
laser ablation (LA)	• *Element to calcium ratios, e.g. Mg/Ca, Sr/Ca* • *Analyse solid samples*	• *Spatial resolution* • *Less destructive than ICP approach* • *Data are comparable*	• *Spatial resolution of > 5 µm, less than SIMS* • *Less sensitive than ICP approach*
Analytical electron microscopy (AEM) with energy dispersive X-ray spectrometry (EDS)	• *Element to calcium ratios, e.g. Mg/Ca, Sr/Ca* • *Microanalysis provides a compositional map with spatial resolution*	• *Low cost and accessible* • *Spatial resolution* • *Non-destructive to specimen surface, therefore can be followed by EBSD, LA-ICP-MS or nanoindentation*	• *Requires elemental standards* • *Detection level at 1000 ppm*
AEM with wavelength-dispersive X-ray spectroscopy (WDS)		• *Moderate cost* • *Nanometer-scale resolution*	• *More costly than AEM-EDS*
Structured illumination microscopy (SIMS)		• *Spatial resolution of SEM* • *Detection sensitivity of 1ppm*	• *High cost* • *Destructive to the sampling area of the specimen*

Electron energy loss spectrometry (EELS)		• *10 ppm detection limit* • *High resolution compositional map*	• *High cost* • *Require 10 nm thick samples* • *Small region of interest*

1473

3. Biomineralisation mechanisms to enable growth (cont.)			
Mineral composition analyses			
Technique	***Measurement(s)***	***Advantages***	***Disadvantages***
Fourier transform infrared spectroscopy (FTIR)	• *Intensity ratio ($I_{max}v_2/I_{max}v_4$) between the absorption bands* • *Identifies the presence of aragonite or calcite*	• *Low cost* • *Provides a comparable measurement of ACC* • *Requires ~1 mg of mineral sample*	• *Semi-quantitative* • *No spatial resolution* • *Destructive*
X-ray diffraction (XRD)	• *Identifies the presence of aragonite or calcite*	• *Allows for quantification of calcite and aragonite ratios* • *Peak position suggests Mg content* • *Powdered sample can be acid-digested to provide elemental data*	• *Requires more powdered samples than FTIR* • *No spatial resolution* • *Destructive* • *Quantitative measurement requires the addition of CaF_2 as an internal standard*
Raman spectroscopy	• *Identifies the distribution of aragonite or calcite*	• *Spatial resolution* • *Area of calcite and aragonite is quantifiable* • *Specimen surface can be analysed by SEM and AEM methods for ultrastructure and elemental contents*	• *Requires sectional surfaces* • *Bleaching is necessary to remove organic contaminants* • *Limited spatial resolution*
SEM-EBSD	• *Identifies the distribution of calcite and aragonite*	• *Allows visual comparison of mineral crystals*	• *Requires fine polishing*

	• *High resolution crystallographic orientation data*	• *Provides quantifiable data on thickness of polymorphs* • *Spatial resolution*	• *Sectional axis and plane of observation must be standardised* • *Moderate cost*

1474

1475

1476

3. Biomineralisation mechanisms to enable growth (cont.)			
Mineral composition analyses (cont.)			
Technique	***Measurement(s)***	***Advantages***	***Disadvantages***
X-ray photo emission electron microscopy (XPEEM) *X-ray atomic spectroscopy (XAS)* *X-ray absorption near edge structure (XANES)*	• *High-spatial resolution composition map* • *Localises and characterises ACC* • *Identify mineral phases*	• *High spatial resolution* • *Sample preparation enables SEM observation and SEM-EBSD characterisation*	• *High cost* • *Requires fine polishing* • *Time-consuming*
Atomic force microscopy (AFM)	• *Records force-distance curve* • *Visualises fine topographical features*	• *Nanometre resolution* • *Simple sample preparation* • *Possible to measure hydrated samples in electrolyte solution*	• *High cost* • *Small area of interest* • *Time-consuming*
Focused ion beam Transmission electron microscopy FIB-TEM	• *Fine spatial resolution* • *FIB prepares TEM sections*	• *Selective region of interest* • *High spatial resolution* • *Suitable for small samples*	• *High cost* • *Time-consuming* • *Small area of interest*

Cryo-electron microscopy	• *High resolution study of biological sample after rapid freezing*	• *High resolution* • *Provides information on composition and crystallography*	• *High cost* • *Requires stabilising detergents for structure*
Stable isotopes	• *Detection of stable isotopes, e.g. δ13C, δ18O, 10B and δ11B*	• *Data are comparable* • *Measures changes in metabolic activity in biomineralisation*	• *Destructive* • *Some proxies are not well established*
Radioactive isotopes	• *Calcification rate* • *Labelling with radioactive isotopes, e.g. ^{45}Ca and ^{14}C*	• *Sensitive technique* • *Specific to experimental exposure*	• *Continual spiking of radiotracer required during incubation* • *Destructive*

1477
1478

4. Cellular biomineralization mechanisms			
Technique	***Measurement(s)***	***Advantages***	***Disadvantages***
SDS-PAGE and MS	• *Characterises shell proteins*	• *Established protocol for protein identification* • *Low cost and high throughput of samples*	• *Sensitivity insufficient to detect shell proteins occurring at low quantity* • *Protein extraction and purification is time consuming* • *Difficult to interpret sequences from non-model marine organisms*
Insoluble organic component analysis using X-ray diffraction (XRD)	• *Characteristic spectroscopy correlated to chitin*	• *Provides evidence on the presence of chitin* • *Analyses insoluble solid samples*	• *Destructive* • *Sufficient sample is hard to obtain* • *Information has poor relevance to the cells and tissue associate with chitin*
Insoluble organic component analysis using infra-red (IR) spectroscopy			

Pyrolysis NMR gas chromatography–mass spectrometry (GC-MS)	• *Detects decomposition product of chitin after chitinase action*	• *Analyses the digested products* • *Digested product peaks can be quantified and compared*	• *Requires chemical standards of digested products* • *Protocol optimisation can be time-consuming*
Colorimetric Assay for acid hydrolysate of chitin	• *Detects decomposition product of chitin after acid hydrolysis*	• *Low cost* • *Quantitative* • *Simple protocol*	• *Destructive* • *Cannot distinguish forms of chitin* • *Spatial information is lost*
Calcofluor-white	• *Visualises chitin in relation to cells and tissues*	• *Non-destructive to tissues and cells* • *Low cost* • *Commercially available*	• *Also binds to cellulose*
Wheat-germ agglutinin (WGA)			• *Also binds to N-acetyl-D-glucosamine and sialic acid*
Chitin-binding domain fused with green fluorescent protein (CBD-GFP)		• *Non-destructive to tissues and cells* • *Specific to chitin*	• *Requires a time-consuming bioengineering approach to express and purify CBD-GFP*

1479

1480

4. Cellular biomineralization mechanisms (cont.)			
Technique	***Measurement(s)***	***Advantages***	***Disadvantages***
OMICS – transcriptomics	• *mRNA of expressed genes*	• *Assesses the molecular pathways of the organism from expressed genes or proteins* • *Provides a whole physiological picture*	• *mRNA presence may not represent protein activities* • *Tissue-specific response* • *Costly* • *Identification of transcripts in a non-model marine species is difficult*
OMICS – proteomics	• *Total protein profile*		• *Shell proteins occurring at low quantity of 5%* • *High-sensitivity method like iTRAQ is very costly*

			• *Identification of protein in a non-model marine species is difficult*
Cellular pH imaging	• *Intracellular pH indicated by a pH sensitive ratiometric probe* • *Visualises the sites of biomineralisation*	• *Examines living organisms* • *High spatial resolution*	• *Not well established and optimisation* • *Ratiometric pH probes require calibration*
Physiological inhibitors and stimulators	• *Enables examination of the physiological response of a non-model organism* • *The importance of a biological pathway is evaluated by a specific inhibitor*	• *Applies to non-model organisms*	• *Some inhibitors are not specific to a single pathway* • *Action of inhibitors should be verified by a known physiological measurement*

1481

1482